

An integrated method for clustering and association network inference

Jeanne Tous^a, Julien Chiquet^a

^aUMR MIA Paris-Saclay, Université Paris-Saclay, AgroParisTech, INRAE, Palaiseau, 91120, France

Abstract

We consider high dimensional Gaussian graphical models inference. These models provide a rigorous framework to describe a network of statistical dependencies between entities, such as genes in genomic regulation studies or species in ecology. Penalized methods, including the standard Graphical-Lasso, are well-known approaches to infer the parameters of these models. As the number of variables in the model (of entities in the network) grow, the network inference and interpretation become more complex. We propose Normal-Block, a new model that clusters variables and consider a network at the cluster level. Normal-Block both adds structure to the network and reduces its size. We build on Graphical-Lasso to add a penalty on the network's edges and limit the detection of spurious dependencies, we also propose a zero-inflated version of the model to account for real-world data properties. For the inference procedure, we propose a direct heuristic method and another more rigorous one that simultaneously infers the clustering of variables and the association network between clusters, using a penalized variational Expectation-Maximization approach. An implementation of the model in R, in a package called **normalblockr**, is available on github (<https://github.com/jeannetous/normalblockr>). We present the results in terms of clustering and network inference using both simulated data and various types of real-world data (proteomics, words occurrences on webpages, and microbiota distribution).

Keywords: Gaussian graphical models, sparse networks, Graphical-Lasso, variational inference, clustering

1. Introduction

In statistics, association networks commonly refer to networks used to describe dependency structures between entities. These entities are represented as nodes, and an edge drawn between two nodes indicates a dependency, whose precise meaning is context-dependent. They can be used in psychological science (Borsboom et al., 2021) or to represent regulation systems in genomics (Fiers et al., 2018; Lingjærde et al., 2021), bacterial associations in biology (Loftus et al., 2021) or species associations in ecology (Ohlmann et al., 2018). They can be both very informative and complex to analyse as the number of nodes and edges they are made of grows.

Undirected graphical models (Lauritzen, 1996; Koller et al., 2007; Whittaker, 2009) are a convenient and rigorous class of models to represent such networks. In this framework, two nodes are joined by an edge if and only if the random variables they represent are conditionally dependent, given all other nodes of the network. Gaussian graphical models (GGM) enter into this framework. They consider a multivariate Gaussian vector so that partial correlations,

and thus the association network, are given by the vectors' precision matrix (the inverse of the variance-covariance matrix). Therefore, the network is described by the model's precision matrix, and its structure corresponds to the support of that matrix.

In practice, a GGM's parameters are typically not directly observed. Instead, they need to be estimated from multiple observations of the multivariate Gaussian vector the model describes. Methods have been developed to infer a sparse network from such observations, so as to select the most meaningful edges in the network. A first category of methods consists in multiple testing, to test the presence of each edge individually (Drton and Perlman, 2007). The most widespread approaches are penalized methods (Yuan and Lin, 2007; Banerjee et al., 2008): they consist in applying a penalty, often an ℓ_1 penalty, to the non-diagonal elements of the precision matrix. This leads some of the non-diagonal terms of the precision matrix to be estimated as zero, which translates into the absence of an edge in the graph. This method thus allows to avoid detecting spurious associations (that is, unestablished dependencies). Graphical-Lasso (Friedman et al., 2008) is the most popular implementation of the ℓ_1 -penalized approach. Methods with different penalties also exist (Chiong and Moon, 2018) as well as more recent approaches that make use of neural networks (Belilovsky et al., 2017) but Graphical-Lasso remains the main reference for inference of sparse networks in GGM. These approaches can also be extended to non-Gaussian data (Chiquet et al., 2019; Liang, 2023) but in this paper, we will stick to the Gaussian framework.

As the number of analysed entities grow, the resulting networks become increasingly hard to infer, requiring more data. Large networks are also more complex to analyse both from a computational point of view and for the interpretation of the results. Metrics exist to aggregate information over the whole network such as connectance, nestedness or associations strength (Soares et al., 2017; Lau et al., 2017). However, such metrics offer very low-grain analysis compared to the complexity of the initial objects they are extracted from. Moreover, they only offer *a posteriori* solutions for the network analysis but they do not reduce the computational cost that comes with Graphical-Lasso inference (Mazumder and Hastie, 2012). Nor do they address the fact, that Graphical-Lasso does not make any *a priori* hypothesis on the network structure, even though real networks are usually not Erdős-Rényi graphs, that is edges do not all have the same probability to appear in the network.

In order to overcome the computational cost of network inference, Meinshausen and Bühlmann (2006) proposed to split the inference into several sub-tasks, using Lasso to infer the neighbourhood of each node in the graph. However, it does not retrieve the variables' individual variance so that one cannot use it to completely retrieve the GGM parameters. Tan et al. (2015) consider Graphical-Lasso as a two-step process – inference of connected components within the graph, and maximization of a penalized log-likelihood on each connected component – and build on this view to propose another version of the Graphical-Lasso that adds some structure in the network through clustering of the variables and reduces the computational cost by applying the Graphical-Lasso separately in each cluster.

Other approaches aim at addressing the issue of the absence of hypothesis on the network structure by identifying or imposing patterns. This can be useful to facilitate network inference, make more hypotheses on its structure and drive the result's interpretation. One can use prior knowledge on the network so as to guide its inference, for instance by forbidding some associations to appear (Grechkin et al., 2015). Another method is to assume an underlying structure in the graph, for instance supposing that some nodes display "hub" roles in the network (Tan et al., 2014), or that edges mostly appear within clusters (Ambroise et al., 2009).

Sanou et al. (2023) propose an approach based on Meinshausen and Bühlmann (2006) and fused-lasso (Pelckmans et al., 2005; Hocking et al., 2011; Lindsten et al., 2011) that estimates

a hierarchical clustering on the variables and a network structure between the clusters. Since it uses the approach of Meinshausen and Bühlmann (2006), this model does not retrieve individual variables' variances. Moreover, the fused-lasso method encourages the inference procedure to retrieve similar dependencies for the elements of the same cluster but it does not directly reduce the size of the network.

Here, we propose the novel Normal-Block model: a Gaussian Graphical Model with a latent clustering structure on the variables and a network defined at the scale of these clusters. As in other approaches (Ambroise et al., 2009; Tan et al., 2015), we assume that the variables belong to hidden clusters that influence the network structure. The novelty of our method is that we consider a network whose nodes are the clusters (and not the variables themselves). This reduces the dimension of the network so as to simplify both the network's analysis and its inference. The model can also account for the effect of external covariates. For the inference, a first heuristic approach consists in using a multivariate Gaussian model on the data. The resulting precision matrix gives a network at the variables level. A clustering of the variables can be done based on the model's residuals. Finally a network at cluster level can be built based on the variables-level network and the clustering. We propose a more ambitious approach that simultaneously clusters the variables and infers the network between the clusters. To this end we resort to variational expectation-maximization to optimize a penalized expected lower-bound of the likelihood. This allows the clustering and the network inference to mutually provide information about one another. We also provide theoretical guarantees on the model's identifiability and inference procedure. Finally, we offer to extend the model to zero-inflated data.

We introduce the Normal-Block model in Section 2 and the corresponding inference strategy in Section 3. In Section 4, we show how the model can be extended to zero-inflated data. In Section 5, we study the results we obtain with simulations. Finally, we illustrate the results of the model and its variants (with and without sparsity or zero-inflation) on real-world data with applications to proteomics data, words occurrences data on web pages and to animal microbiological species in Section 6.

Notations. Throughout the paper, \odot shall denote the Hadamard product, \otimes the Kronecker product. For a matrix A and an integer b , A^b shall denote the matrix with same dimensions as A obtained by individually raising each element of A to the power of b , and A° the term-to-term inverse of A . Similarly $f(A)$ will correspond to the term-to-term application of function f to matrix A . We use $\bar{A} = (\sum_i A_i)^T$, $\underline{A} = \sum_j A_{.j}$ and $\underline{\underline{A}} = \sum_{ij} A_{ij}$

2. An integrated model of clustering and network reconstruction for continuous data

2.1. Normal-Block model

We observe $\{Y_i, 1 \leq i \leq n\}$, n realizations of a p -dimensional Gaussian vector so that Y_i may describe the expression intensities of p genes in cell i or the biomass of p species in site i .

The model relates each continuous vector $Y_i \in \mathbb{R}^p$ ($1 \leq i \leq n$) to a vector of latent variables of smaller dimension $W_i \in \mathbb{R}^Q$, $Q < p$, with precision matrix Ω_Q (that is, covariance matrix $\Sigma_Q = \Omega_Q^{-1}$). As in a multivariate linear model, we also include the effects of a combination of covariates $X_i \in \mathbb{R}^d$, with $d \times p$ matrix B , the matrix of regression coefficients.

$$\begin{aligned} \text{Latent space: } W_i &\sim \mathcal{N}(0, \Omega_Q^{-1}) \\ \text{Observation space: } Y_i | W_i &\sim \mathcal{N}(CW_i + X_i B, D) \end{aligned} \tag{1}$$

We denote the observed matrices by Y and X , with sizes $n \times p$, $n \times d$ stacking vectors row-wise, and W the $n \times Q$ matrix of latent Gaussian vectors. The $p \times Q$ matrix C is a clustering matrix with $C_{jq} = 1$ if and only if entity j belongs to cluster q . This clustering links observations Y_i and latent variables W_i . C can either be observed or not. When C is observed, the framework of Model (1) is that of multivariate mixed models, with B a matrix of fixed effects with design matrix X , and W a matrix of random effects with C being the corresponding design matrix. When C is unobserved, we further assume that each $C_j \in \{0, 1\}^Q$ is a multinomial random variable, that is: $C_j \sim \mathcal{M}(1, (\alpha_{jq})_{1 \leq q \leq Q})$ so that $\sum_{q=1}^Q \alpha_{jq} = 1$.

Model (1) relates observations Y_i both to observed covariates X and to a clustering effect that translates into W_i 's covariance. The addition of a diagonal variance matrix D in the conditional distribution of Y aims at separating the effect of variables' individual variance to ensure that the clusters' effects on covariances is not biased by individual variance effects. We can also consider a spherical model, forcing individual variances to be the same for each entity so that D becomes a spherical variance matrix: $D = \text{diag}(\xi^{-1})$, $\xi \in \mathbb{R}^{+*}$. The set of model parameters is denoted as $\theta = (B, \Omega_Q, D)$.

This framework allows the modelling of small networks (of size $Q \times Q$) from large datasets, based on a clustering of the entities, as we detail in Section 2.2.

2.2. Graphical model

The goal of the model is to consider a clustering (whether it is observed or not) of continuous variables and an association network between the clusters. To do so, we resort to the framework of graphical models (Lauritzen, 1996). The association network encodes the dependencies between the components of the latent variable W , corresponding to the observations Y 's residuals after accounting for covariates. More precisely, variables W_q and W_k are connected in the graph if they remain dependent after conditioning on all other W_j . Since the W are jointly Gaussian, this dependence corresponds to a non-zero value in the precision matrix Ω_Q of the Gaussian distribution, that is: W_q and W_k are connected in the network if and only if $\Omega_{Q_{qk}} \neq 0$. The partial correlation between them is then given by $-\Omega_{Q_{qk}} / \sqrt{\Omega_{Q_{qq}} \Omega_{Q_{kk}}}$. Thus, the association network between the Q clusters is represented in the dependency structure between the components of the latent variable W_i from one site i to another, and it is encoded in W_i 's precision matrix Ω_Q of size $Q \times Q$.

The structure of the network is determined by the support of Ω . To limit the detection of spurious associations, we may want to infer a sparse network. To do so, we add an ℓ_1 penalty on Ω_Q in the likelihood or its variational approximation in the inference procedure. We resort to Graphical-Lasso to implement this regularization (Friedman et al., 2008).

2.3. Identifiability

In this section, we explain that the Normal-Block model with observed clusters is identifiable, under mild conditions. Extension of the proof to the model with unobserved clusters seem much more complex to achieve.

Proposition 2.1. *The spherical Normal-Block model with observed clusters is identifiable provided X has rank d , no cluster is empty and at least one cluster contains at least two elements.*

Proposition 2.2. *The Normal-Block model with observed clusters is identifiable provided X has rank d and each cluster contains at least two elements.*

The proofs for both propositions are presented in Appendix A.

Remark. *These propositions express the intuitive idea that the variables' variances is a mix of their cluster's variance and their individual variance. If the group is only made of one element then these two variances represent the same thing. In the spherical model case the hypothesis is less constraining because the individual variances are assumed to be the same for all.*

Remark. *Should the hypothesis on the number of elements in each cluster not be respected, the model's interpretation would not be hindered. Indeed if cluster q contains only category j , one would simply need to consider the sum $\Sigma_{Q,q} + D_{jj}$ as both the cluster and individual variance, since they both correspond to the same entity.*

When the clusters are unobserved, the identifiability becomes much more complex to prove. Indeed, the marginal likelihood becomes:

$$p_{\theta}(Y_i) = \sum_{C^* \in \{1;Q\}^p} \left(\prod_{j=1}^p \alpha_{C_j^*} \right) \mathcal{N}(B^T X_i, D + C^* \Sigma_Q C^{*\top})$$

We have not yet explored the possible proof for the identifiability in that case. Leads for such a proof could be found in Allman et al. (2009, 2011) or Matias and Miele (2017). From an empirical point of view, in the simulations we ran, the correct clustering was usually very well retrieved so that the identifiability results for the observed-clusters model might still hold empirically.

3. Inference strategy

We now describe the inference strategies, which aim at estimating B, Ω_Q, D (or ξ in the spherical model), and, when not observed, C . We first introduce a heuristic, straightforward method in multiple steps (3.1) before proposing a more rigorous approach (3.2, 3.3) relying on Expectation-Maximization (EM) when clusters are observed and on Variational EM when they are not, simultaneously inferring the clustering and the network. Finally, we discuss model selection in Section 3.4.

3.1. Heuristic method

To infer the model's parameters, a first straightforward approach relies on a simple multiple-step procedure described herein. Consider the Gaussian multivariate linear model

$$Y_i = B^T X_i + R_i, \text{ with } R_i \sim \mathcal{N}(0, \Sigma), \quad (2)$$

with Σ a $p \times p$ covariance matrix. For B and Σ , we use the standard multivariate linear regression estimators: $\hat{B} = (X^T X)^{-1} X^T Y$, $\hat{R} = Y - X \hat{B}$ and $\hat{\Sigma} = \hat{R}^T \hat{R} / n$.

Then, if clustering C is not observed, we either estimate it with a k-means algorithm on \hat{R} , or with a stochastic block model (SBM) (Holland et al., 1983; Chiquet et al., 2024) on $\hat{\Sigma}$. Once we have a clustering C (observed or estimated), the empirical $Q \times Q$ covariance $\tilde{\Sigma}_Q$ between groups is estimated with

$$\tilde{\Sigma}_{Q_{q_1, q_2}} = \frac{1}{|q_1| \times |q_2|} \sum_{j_1, j_2, C_{j_1} C_{j_2} = 1} \hat{\Sigma}_{j_1, j_2}$$

where $|q_1|, |q_2|$ are the number of elements in clusters q_1 and q_2 respectively.

Finally, the sparse estimator of Σ_Q is obtained by applying Graphical-Lasso to $\tilde{\Sigma}_Q$. We use the implementation provided in the package **glassoFast** (Sustik and Calderhead, 2012).

The primary benefit of this method is its simplicity and intuitiveness. Additionally, its outcomes can serve as an initial input for our more elaborate, integrated inference approach. However, the heuristic method lacks rigorous justification and cannot estimate all model parameters (particularly D) because it does not optimize a specific criterion like the likelihood. This limitation makes it difficult to assess the model's fit to the data and prevents the development of a statistically sound criterion for selecting the number of groups or edges in the network. Furthermore, this method infers the network and clustering separately. It first retrieves a network at the variable level, which does not reduce dimensionality and thus fails to address computational challenges. Additionally, handling clustering separately prevents the two processes from informing each other. Therefore, in the subsequent sections, we propose a more rigorous approach that simultaneously infers both the clustering and the network at the cluster level.

3.2. Expectation-Maximization method for the observed clusters model

We now introduce a fully integrated likelihood-based approach to infer the model parameters $\theta = (B, \Omega_Q, D)$. We first consider the inference when the clustering is observed.

If C is given and fixed, we can write the marginal distribution of Y_i :

$$Y_i \sim \mathcal{N}(B^T X_i, \Sigma) \text{ with } \Sigma = D + C\Omega_Q C^T.$$

However, the marginal likelihood does not allow one to tease apart the effects of D and $C\Omega_Q C^T$ in the variance. Thus we instead resort to the complete likelihood $\log p(Y_i, W_i)$, using an Expectation Maximization (EM) strategy (Dempster et al., 1977).

The E step consists in evaluating the conditional expectation $\mathbb{E}_{W_i \sim p(\cdot | Y_i, \theta)}[\log p_\theta(Y_i, W_i)]$, which requires the characterization of the posterior distribution $W_i | Y_i$. Since W_i and Y_i are both Gaussian variables, we can explicitly develop the expression of the conditional density using Bayes formula and we get

$$W_i | Y_i \sim \mathcal{N}(\mu_i, \Gamma), \quad \text{with } \Gamma = (C^T D^{-1} C + \Omega_Q)^{-1} \text{ and } \mu_i = \Gamma C^T D^{-1} (Y_i - B^T X_i).$$

Then, we easily derive the expression for the EM criterion, which serves as our objective function in θ from an optimization standpoint:

$$\begin{aligned} J(\theta) = & -\frac{np}{2} \log(2\pi) - \frac{n}{2} \log \det(D) - \frac{1}{2} \text{tr} \left(D^{-1} (R_\mu^T R_\mu + n C \Gamma C^T) \right) \\ & - \frac{nQ}{2} \log(2\pi) + \frac{n}{2} \log \det(\Omega_Q) - \frac{1}{2} \text{tr} \left(\Omega_Q (n \Gamma + \mu^T \mu) \right) \end{aligned}$$

with $R_\mu = Y - XB - \mu C^T$ and μ the matrix whose rows are the μ_i^T , that is $\mu^T = \Gamma C^T D^{-1} (Y - B^T X)$.

The M-step consists in updating the parameters by maximizing J w.r.t θ . Closed-forms are obtained for the different parameters (B, Ω_Q, D) by differentiation of the objective function $J(\theta)$, so that the concavity, at least in each parameter, is needed. This is stated in the following Proposition, the proof of which is presented in Appendix B.

Proposition 3.1. *In the observed-clusters model, the objective function J is jointly concave in (Ω_Q, D^{-1}) and in (Ω_Q, B) . The same holds for the spherical model, with joint concavity in (Ω_Q, ξ^{-1}) and in (Ω_Q, B) .*

We now state the closed-form expressions for the estimators calculated during the M-step:

Proposition 3.2. *The M-estimators for the observed-clusters model, obtained by differentiation of J w.r.t. B, Σ_Q, d the diagonal vector of D and ξ for the spherical model are given by*

$$\begin{aligned}\hat{B} &= (X^T X)^{-1} X^T (Y - \mu C^T), \quad \hat{\Sigma}_Q = \frac{1}{n} \mu^T \mu + \Gamma, \\ \hat{d} &= \overline{R_\mu^2}/n + C \text{diag}(\Gamma), \quad \hat{\xi}^2 = \overline{R_\mu^2}/np + \overline{C}^T \text{diag}(\Gamma)/p.\end{aligned}$$

As mentioned in Section 2.2, we may also want to add an ℓ_1 penalty on Ω_Q so as to infer a sparse network structure. In that case, the objective function becomes $J_{\text{struct}} = J - \lambda \|\Omega_Q\|_{\ell_1, \text{off}}$, where $\|\Omega_Q\|_{\ell_1, \text{off}}$ is the off-diagonal ℓ_1 norm of Ω_Q and $\lambda > 0$ is a tuning parameter to control the sparsity level. We only penalize the off-diagonal element of Ω_Q since we only want to restrict the associations, not the intra-clusters variances. J_{struct} is a lower bound of J , whether the clusters are observed or not. Thanks to the concavity of $\Omega_Q \mapsto -\lambda \|\Omega_Q\|_{\ell_1, \text{off}}$, adding the penalty does not change the structure of the objective function, which preserves its concavity property:

Corollary 3.1.1. *In the observed-clusters diagonal and spherical models, the penalized objective function J_{struct} is jointly concave in (Ω_Q, D^{-1}) and in (Ω_Q, B) .*

The E-step and M-step are similar in the sparse case: we evaluate $J_{\text{struct}}(\theta)$ and estimate the model parameters as stated in Theorem 3.2. The only striking difference lies in the estimation of Ω_Q , obtained here with Graphical-Lasso applied to $\hat{\Sigma}_Q$. We use the implementation provided in the package **glassoFast** (Sustik and Calderhead, 2012).

The whole EM algorithm is initialized with the heuristic method described in Section 3.1, from which we obtain starting values for the parameters B and Σ_Q . The rest of the optimization then consists in alternately updating the parameters of the posterior distribution (Γ, μ) in the E-step and, and of the model parameters (B, D, Ω_Q) in the M-step.

3.3. Variational inference for the unobserved clusters method

When the clustering C is not observed, we can also propose an integrated inference method, allowing the clustering and the network at cluster level to simultaneously be inferred. We assume that the number of clusters Q is fixed as a hyper-parameter. The marginal likelihood can no longer be computed so that we also need to resort to an EM strategy. However, this requires computing some moments of $W, C \mid Y$ since they are required in the E step for the evaluation of $\mathbb{E}_{C, W_i \sim p(\cdot \mid Y; \theta)}[\log p_\theta(Y_i, W_i, C)]$. Since these posterior distribution moments are untractable, we resort to a variational approximation (Blei et al., 2017; Wainwright and Jordan, 2008) and proceed with a Variational-EM (VEM) algorithm.

3.3.1. Variational approximation

Under the variational approximation, we assume that:

$$\begin{aligned}\mathbb{P}(W, C \mid Y) &\sim \mathbb{P}(W \mid Y) \mathbb{P}(C \mid Y) \\ &\sim \prod_{i=1}^n \mathbb{P}(W_i \mid Y) \prod_{j=1}^p \mathbb{P}(C_j \mid Y) \\ &\sim \prod_{i=1}^n \pi_1(W_i) \prod_{j=1}^p \pi_2(C_j)\end{aligned}$$

with:

- π_1 the approximation for $W|Y$: $W_i \sim^{\pi_1} \mathcal{N}(M_i, S_i)$, S_i being diagonal. We denote $S \in \mathcal{M}_{n,Q}(\mathbb{R})$ defined by $S_{i,q} = s_{i,q}$ and $M \in \mathcal{M}_{n,Q}(\mathbb{R})$ defined by $M_{i,q} = M_{i,q}$ so that the parameters of π_1 can be denoted $\psi_1 = (M, S)$.
- π_2 the approximation for $C|Y$: $C_j \sim^{\pi_2} \mathcal{M}(1, (\tau_{jq})_{1 \leq q \leq Q})$ and $\forall j \in \llbracket 1; p \rrbracket$, $\sum_{q=1}^Q \tau_{jq} = 1$. We denote $\tau \in \mathcal{M}_{p,Q}(\mathbb{R})$ the matrix of $(\tau_{jq})_{j \in \llbracket 1; p \rrbracket, q \in \llbracket 1; Q \rrbracket}$ so that the parameters of π_2 can be denoted $\psi_2 = (\tau)$.

The quality of this approximation is measured with the Kullback-Leibler divergence between the two distributions (that is, the true, untractable $W, C|Y$ and the distribution $\pi_1 \pi_2$). This allows us to write a variational lower-bound (ELBO or Expected Lower Bound) of the marginal log-likelihood:

$$\begin{aligned}
J &= \log p_\theta(Y) - KL[\pi_1(W)\pi_2(C)|Y||p_\theta(W, C|Y)] \\
&= \mathbb{E}_\pi(\log p_\theta(Y, W, C)) - \mathbb{E}_{\pi_1}(\log \pi_1(W)) - \mathbb{E}_{\pi_2}(\log \pi_2(C)) \\
&= -\frac{n}{2} \log(2\pi) - \frac{n}{2} \log(\det(D)) - \frac{1}{2} \mathbf{1}_n^T (AD^{-1}) \mathbf{1}_p \\
&\quad - \frac{nQ}{2} \log(2\pi) + \frac{n}{2} \log \det(\Omega_Q) - \frac{1}{2} \text{tr}(\Omega_Q(\text{diag}(\bar{S}) + M^T M)) \\
&\quad + \frac{nQ}{2} \log(2\pi e) + \frac{1}{2} \mathbf{1}_n^T \log(S) \mathbf{1}_Q + \mathbf{1}_p^T \tau \log(\alpha) - \mathbf{1}_p^T ((\tau \odot \log(\tau))) \mathbf{1}_Q,
\end{aligned}$$

where $R = Y - XB$ and $A = R^2 - 2R \circ M\tau^T + (M^2 + S)\tau^T$, and $\bar{S} = \sum_{i=1}^n S_i$.

3.3.2. Concavity

Proposition 3.2. *In the unobserved-clusters model the objective function J is individually concave in each of its terms.*

A proof of this proposition is presented in Appendix B. We do not have the global concavity of J so that its convergence towards a global optimum is not guaranteed.

Corollary 3.2.1. *In the unobserved-clusters model the penalized objective function J_{struct} is individually concave in each of its terms.*

This corollary arises from the concavity of $\Omega_Q \mapsto -\lambda \|\Omega_Q\|_{\ell_1, \text{off}}$.

3.3.3. Inference algorithm

Similarly to the observed clusters case, the VEM algorithm consists in alternately computing estimators for the variational parameters M, S, τ in the VE-step and for the model parameters α, B, D, Ω_Q in the M-step. First-order derivatives of the ELBO give explicit estimators for all of these parameters. The expressions obtained thereby are given in Proposition 3.3.

Proposition 3.3. *In the unobserved-clusters case, estimators of the variational parameters in the E-step are*

$$\hat{M} = RD^{-1} \tau \tilde{\Gamma}, \quad \hat{S}_i = \text{diag}(\tilde{\Gamma}), \quad \hat{\tau}_j = \text{softmax}(\eta_j),$$

where we denote $\tilde{\Gamma} = (\Omega_Q + \text{Diag}(\tau^T d^{-1}))^{-1}$ and $\eta = -\frac{1}{2}d^{-1} \otimes (\overline{M^2} + nS_i) + D^{-1}R^T M + \mathbf{1}_p \otimes \log(\alpha) - 1$.

For the M -step, we have

$$\hat{B} = (X^T X)^{-1} X^T (Y - M\tau^T), \quad \hat{\Sigma}_Q = \frac{1}{n}(M^T M + \text{Diag}(\overline{S})), \quad \hat{d} = \frac{1}{n}\overline{A},$$

denoting $A = R^2 - 2R \circ M\tau^T + (M^2 + S)\tau^T$.

For the initialization we also need to specify an initial clustering. We still rely on our heuristic approach where, when the clustering is unobserved, we use the k-means algorithm on the residuals of a multivariate Gaussian model or a SBM on the empirical covariance at the variable scale.

3.4. Model selection

There are two underlying hyper-parameters to the Normal-Block model. The first one is the penalty λ applied on the precision matrix: the higher it gets, the sparser is the resulting network. The second one, when the clustering is not observed, is the number of clusters Q . While there is no exact method to fix these two parameters, we propose several approaches here.

3.4.1. Selecting the number of groups

As is often the case in clustering problems, the number of clusters, Q here, is a hyper-parameter. The Bayesian Information Criterion (BIC), the Extended BIC (EBIC) and the Integrated Complete Likelihood (ICL) (Biernacki et al., 2000) can be used as criteria to fix Q . While the model's likelihood increases with Q because the number of parameters does so, these criteria penalize a too important number of parameters and help find a balance. Empirically, on simulated data, with $n \in \{50, 100, 200\}$, $p = 100$ and $Q \in \{3, 5, 10\}$, we find that the BIC and the EBIC retrieve the correct number of clusters in more than 99% cases while the ICL does so in more than 97% of them. When an error is made, the number of clusters identified by the criterion is either equal to $Q + 1$ or $Q - 1$.

3.4.2. Selecting the penalty

Adding a penalty λ on Ω_Q helps infer a sparse network. Several approaches exist to find the optimal λ in GGM. A higher λ will force more values of Ω_Q to 0 and hence reduce the number of parameters and the likelihood while statistical criteria such as the BIC, the ICL or the EBIC (Chen et al., 2008) will favour both an increasing likelihood and a lower number of parameters. One can rely on these criteria to fix λ .

Another approach that we propose is the Stability Approach to Regularization Selection (StARS) (Liu et al., 2010). In short it consists in recomputing networks from data subsamples for each λ and to keep the value of λ for which the networks inferred with the different subsamples are the most stable, stability being measured through the frequency of appearance of the edges in the networks obtained from the different subsamples. As the Normal-Block networks are built at the scale of clusters, we need to fix Q and the clustering to proceed to StARS. For a fixed Q , we propose to keep it as it is when no penalty is applied on the network ($\lambda = 0$). StARS then keeps the lowest penalty such that all the edges it identifies are present in more than $x\%$ of the networks obtained from subsamples, x being a hyper-parameter called stability threshold and taking values between 0 and 1.

We compare the criterion-based approaches and the StARS approach using the F1-score, equal to $2 \times \frac{\text{precision} \times \text{recall}}{\text{precision} + \text{recall}}$ (Figure 1).

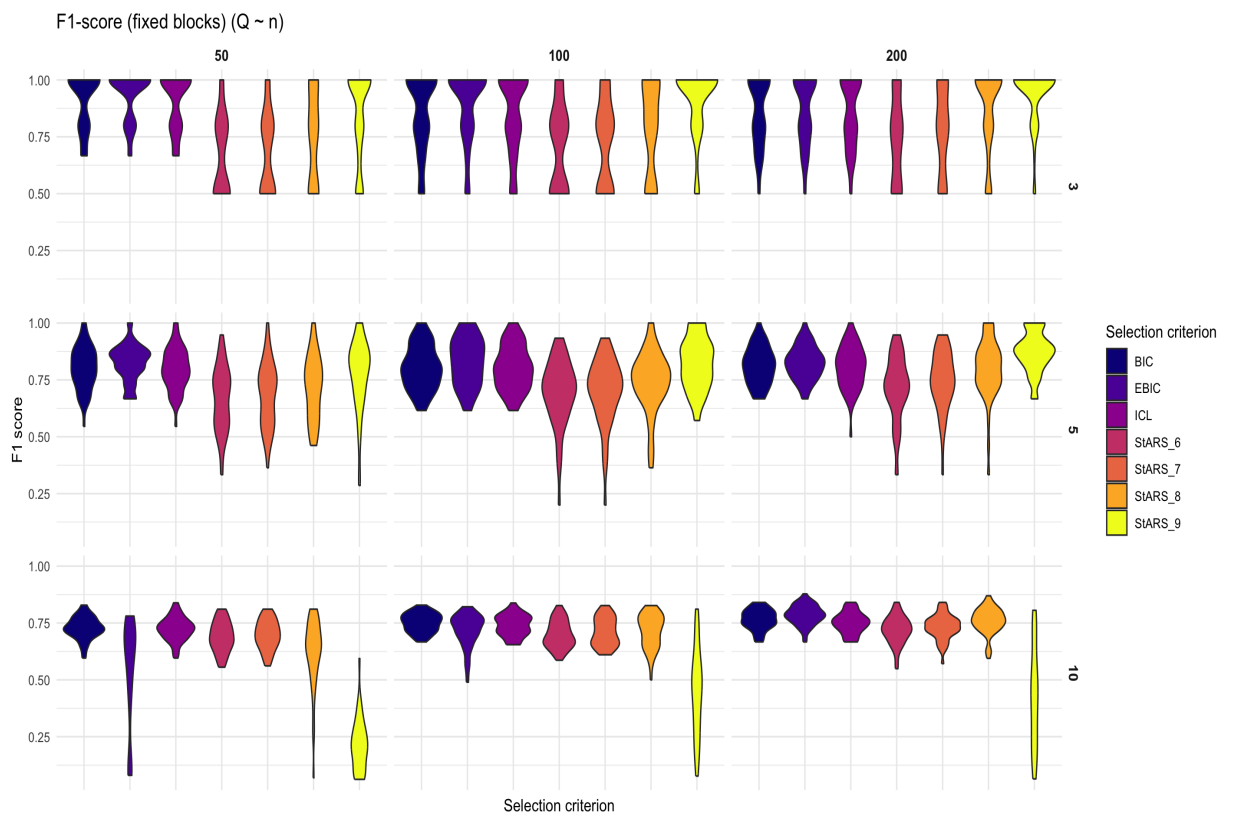


Figure 1: Violin plots of the F1 scores obtained with fixed blocks, for $Q \in \{3, 5, 10\}$ and $n \in \{50, 100, 200\}$ for the penalty retrieved using either BIC, EBIC or ICL criteria, or a StARS method with stability fixed at 0.6, 0.7, 0.8, 0.9.

Figure 1 shows that the three criteria obtain similar results in terms of F1 score. StARS results are much worse when using a stability value that is too high (0.9). For lower stability values, the results are comparable. Overall the BIC, EBIC and ICL criteria seem to offer better results. Moreover, using StARS is computationally expensive due to the resampling procedure so that it seems preferable to resort to one of the statistical criteria.

4. Extension to zero-inflated Gaussian data

Additionally to the model and inference methods we have proposed, we offer to extend the model to zero-inflated data in this section. This can be useful in situations where real-world data display zero-inflated patterns (that is, contains more zeros than can be explained by a Gaussian distribution) whether it is because of technical limitations, variations in sampling efforts or other reasons. This is often the case in ecology due to sampling procedure or in genomics, with single-cell experiments for instance. As in Section 3, we also propose a heuristic method for parameters inference (4.2) and a VEM-based method (4.3).

4.1. Model

For the zero-inflated version of Normal-Block, taking inspiration from Batardière et al. (2024), we add a second latent variable Z , such that each Z_{ij} follows a Bernoulli distribution of parameter κ_j :

$$\begin{aligned} \text{Gaussian latent layer: } W_i &\sim \mathcal{N}(0, \Omega_Q^{-1}) \\ \text{Excess of 0 latent layer: } Z_i &\sim \bigotimes_j \mathcal{B}_j(\kappa_j) \\ \text{Observation space: } Y_i | Z_i, W_i &= Z_i \odot \delta_0 + (1 - Z_i) \odot (C W_i + \mathcal{N}(B^\top X_i, D)) \end{aligned}$$

where δ_0 is the Dirac distribution in 0.

4.2. Heuristic inference method

We propose a multiple-step straightforward inference method. We first infer B and κ as the parameters of a zero-inflated diagonal Normal model, defined as:

$$Y_i | Z_i = \delta_0 Z_i + (1 - Z_i) \mathcal{N}(B^\top X_i, D).$$

For parameter inference, we resort to an EM approach. The model also outputs posterior probabilities that each data point was produced by the zero-inflated component: $\rho_{ij} = p(Z_{ij} = 1 | Y_{ij})$. We can compute residuals $\tilde{R} = Y - X B$ and obtain \hat{R} from \tilde{R} replacing $\tilde{R}_{i,j}$ with 0 when $\rho_{ij} > 0.7$. From here, we compute $\hat{\Sigma} = \hat{R}^\top \hat{R} / n$. As for the non-zero-inflated data (3.1), when the clustering C is not observed, we either infer it with a k-means algorithm on R or a SBM (Holland et al., 1983; Chiquet et al., 2024) on $\hat{\Sigma}$, and from then obtain $\hat{\Sigma}_Q$ the same way.

4.3. VEM-based inference method

For the observed clusters models, computing the marginal log-likelihood or the complete log-likelihood without variational approximation is still feasible, but it requires going through all possible values of Z_i that would yield Y_i , that is, through all elements of $\{(Z_i)_{1 \leq i \leq n} | \forall i \in \llbracket 1; n \rrbracket, Z_{ij} = 1 \rightarrow Y_{ij} = 0\}$, a set of cardinal $2^{\sum_{i,j} 1_{Y_{ij}=0}}$. To avoid the computational burden that comes with such calculations, we proceed to a VEM inference. Again, we resort to a mean-field approximation with $W_i, Z_i | Y_i$ approximated by $\pi_1 \pi_2$ with $W_i \sim^{\pi_1} \mathcal{N}(M_i, S_i)$, S_i being diagonal and $Z_{ij} \sim^{\pi_2} \mathcal{B}(\rho_{ij})$. Details for the corresponding ELBO and estimators are given in Appendix C.

5. Simulation study

We study the performance of our inference methods on data simulated under the Normal-Block model, with and without zero-inflation. The code used to simulate the data is available in the *inst* folder of the **normalblockr** github repository. We first want to test their ability to retrieve the correct clustering when it is not observed, and the structure of the association network (that is, the support of the association matrix). To assess how the network is retrieved, we only consider observed-clusters simulations. Indeed, when clusters are unobserved, the model is only identifiable up to label permutation and comparing the networks require testing all these permutations. As the clustering is usually well-retrieved by the integrated inference method, one can imagine that the results would be similar between observed and unobserved clusters simulations for network inference. More generally, we also test the inference methods' ability to retrieve each parameter's value.

We want to compare these results for different levels of difficulties. We assume that increasing Q and decreasing n make the inference harder as it means more information to retrieve with less signal. Similarly, increasing the level of zero-inflation is likely to degrade the results as it removes some of the signal in the data. We also run simulations for different structures of Ω_Q to see if some network structures are easier to retrieve than others.

5.1. Simulation protocol

5.1.1. Network generation

To generate the ground-truth Ω , we first produce a sparse undirected graph with different possible structures: Erdős-Rényi (no particular structure), preferential attachment (edges are attributed progressively with a probability proportional to the number of edges each node is already involved in) and community (in the Stochastic Block Models sense, Holland et al. (1983)). This allows us to test the robustness of the inference procedure when facing different dependency structures. Using package **igraph** (Csardi and Nepusz, 2006), we generate an adjacency matrix G corresponding to a given structure. Then Ω is created with the same sparsity pattern as G as follows: $\tilde{\Omega} = G \times v$ and $\Omega = \tilde{\Omega} + \text{diag}(\min(\text{eig}(\tilde{\Omega})) + u)$, with $u, v > 0$ two scalars. Higher v means stronger correlations whereas higher u means better conditioning of Ω . Following Chiquet et al. (2019) we fix $v = 0.3, u = 0.4$ in the simulations.

5.1.2. Data generation

We simulate data under the Normal-Block model. We draw a random but balanced clustering (variables are affected to each cluster with equal probability), a unique covariate taking values in $[1; 10]$ then draw Y according to the model. For all simulations we fix the number of variables, p to 50. For non-zero-inflated Normal-Block we test $n = 50, 100$ or 200 , $Q = 3, 5$, or 10 .

Inference for zero-inflated data takes significantly longer, especially as Q increases so that we only test $Q = 3, 5$, $n = 75$ and Erdős-Rényi graph structure, but we test different levels of zero-inflation. κ is drawn from a truncated Gaussian distribution, with standard deviation of $\sigma = 0.05$, mean μ either equal to $0.1, 0.5$ or 0.8 and distribution truncated at 0.9 so as to ensure enough signal remains for each variable for the model to work.

In both the regular and zero-inflated simulations, each configuration is simulated 50 times.

5.1.3. Metrics

We first want to test the inference procedure’s ability to retrieve the model’s clustering. We use the adjusted rand index (ARI), computed with package **aricode** (Rigaill et al., 2020) to compare ground-truth clustering and inferred clustering.

The inference procedure produces a series of network, one for each value of the penalty λ we use for Graphical-Lasso (the higher λ gets, the more 0s $\hat{\Omega}_Q$ contains). In this assessment, we leave aside the issue of choosing λ . Instead, we compare the real and inferred networks with the Receiving Operator Characteristic (ROC) curve and the corresponding Area Under the Curve (AUC). The ROC curve plots the True Positive rate (or recall) as a function of the False Positive rate (or fallout), AUC is the area under that curve. The larger the AUC, the better is the network reconstruction. Since the model does not change when permuting clusters labels, comparing networks with unobserved clusters requires testing the labels permutations, so that we only compute the AUCs in the observed clusters configuration.

To test the model’s ability to correctly retrieve other parameters, we use the root mean squared error (RMSE) for B , D , κ (for zero-inflated data). We also use it for \hat{Y} to assess the inference procedure’s ability to correctly fit the data.

5.1.4. Comparison between inference methods

While we focus on the more elaborate ”simultaneous inference” procedure, we compare its results with those obtained with the heuristic approaches, using two possible clustering methods (SBM on the precision matrix or k-means on the residuals).

5.2. Results

Table 1 shows that both the Normal-Block model and the 2-step methods almost systematically retrieve the correct clustering, for all the network structures that we tested and even when n is significantly lower than $p = 50$.

Figure 2 (A and B) shows that both the integrated and the 2-step method correctly retrieve the network structure. However, we see that as the number of clusters Q increases, the graph structure is harder to retrieve. This is likely owing to the fact that the network size increases whereas the number of variables per cluster does not. We also see that the Erdős-Rényi networks (no particular structure) are harder to retrieve than the more structured ones.

In the case of zero-inflated data, we see that the zero-inflation does not affect the AUC much when the clustering is observed (Figure 2 C). However, increasing the zero-inflation significantly affects the model’s ability to retrieve the correct clustering (Figure 2 D). In terms of ARI, we also see that the 2-step methods’ results are much worse than those of the integrated inference method when the zero-inflation is important.

Figure 3 shows that increasing n reduces the error on the estimates of B and D while it does not improve the quality of the fit. The value of Q does not seem to have a significant impact on these results. In the case of zero-inflated data (Figure 4), an increasing zero-inflation increases the error for B and D while it reduces it for the fitting error. This might be explained by the increasing number of zeros that are correctly predicted. The effect of an increasing zero-inflation on its assessment is not clear but it does not seem to have a significant impact.

6. Illustrations

We show how the different variants of the models can be applied to analyse data from different fields. First we use a simple Normal-Block model for the analysis of proteomics data and

n	Q	Omega structure	Proportion of ARI at 1 - Normal-Block	Mean value of ARI when < 1 - Normal-Block	Proportion of ARI at 1 - 2-step method residuals clustering	Mean value of ARI when < 1 - 2-step method residuals clustering	Proportion of ARI at 1 - 2-step method variance clustering	Mean value of ARI when < 1 - 2-step method variance clustering
50	3	community	1.00		1.00		1.00	
50	3	Erdos Renyi	1.00		1.00		1.00	
50	3	Preferential attachment	1.00		1.00		1.00	
50	5	community	1.00		1.00		0.98	0.98
50	5	Erdos Renyi	1.00		1.00		0.90	0.97
50	5	Preferential attachment	1.00		1.00		1.00	
50	10	community	0.93	0.94	0.95	0.89	0.84	0.95
50	10	Erdos Renyi	0.95	0.95	0.94	0.91	0.68	0.93
50	10	Preferential attachment	0.94	0.93	0.95	0.90	0.78	0.92
100	3	community	1.00		1.00		1.00	
100	3	Erdos Renyi	1.00		1.00		1.00	
100	3	Preferential attachment	1.00		1.00		1.00	
100	5	community	1.00		1.00		1.00	
100	5	Erdos Renyi	1.00		1.00		1.00	
100	5	Preferential attachment	1.00		1.00		1.00	
100	10	community	0.91	0.91	0.94	0.92	0.96	0.98
100	10	Erdos Renyi	0.85	0.94	0.85	0.90	0.98	0.91
100	10	Preferential attachment	0.91	0.93	0.91	0.90	1.00	
200	3	community	1.00		1.00		1.00	
200	3	Erdos Renyi	1.00		1.00		1.00	
200	3	Preferential attachment	1.00		1.00		1.00	
200	5	community	1.00		1.00		1.00	
200	5	Erdos Renyi	1.00		1.00		1.00	
200	5	Preferential attachment	1.00		1.00		1.00	
200	10	community	0.82	0.95	0.90	0.93	1.00	
200	10	Erdos Renyi	0.78	0.93	0.83	0.91	1.00	
200	10	Preferential attachment	0.87	0.94	0.92	0.93	1.00	

Table 1: ARI results for each configuration.

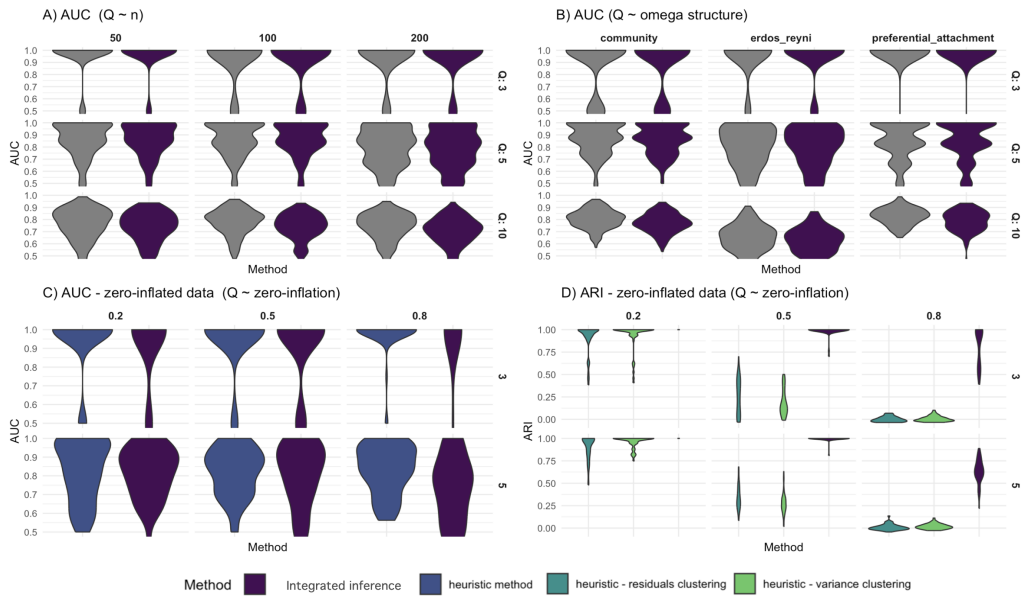


Figure 2: AUC and ARI results for simulated data with / without zero-inflation. A) AUC results for non-zero-inflated data, for different values of Q and n , B) AUC results for non-zero-inflated data, for different values of Q and n and different network structures. C) AUC results for zero-inflated data for different values of Q and different levels of zero-inflation. D) ARI results for zero-inflated data for different values of Q and different levels of zero-inflation (alt is for "alternative", meaning the two-step method).

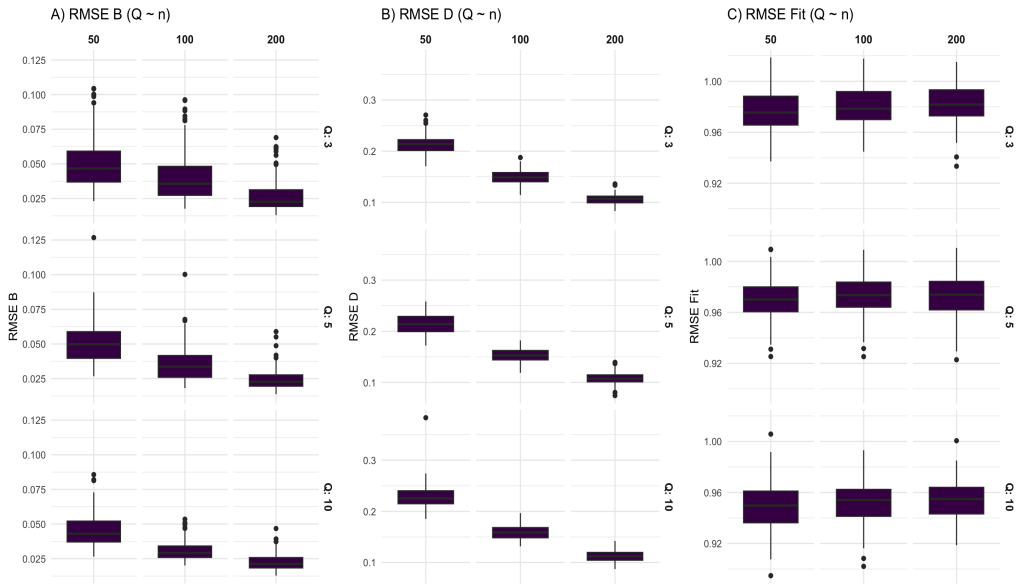


Figure 3: RMSE measured for B (A), D (B) and for real-data fitting (C) for different values of n and Q (non-zero-inflated data).

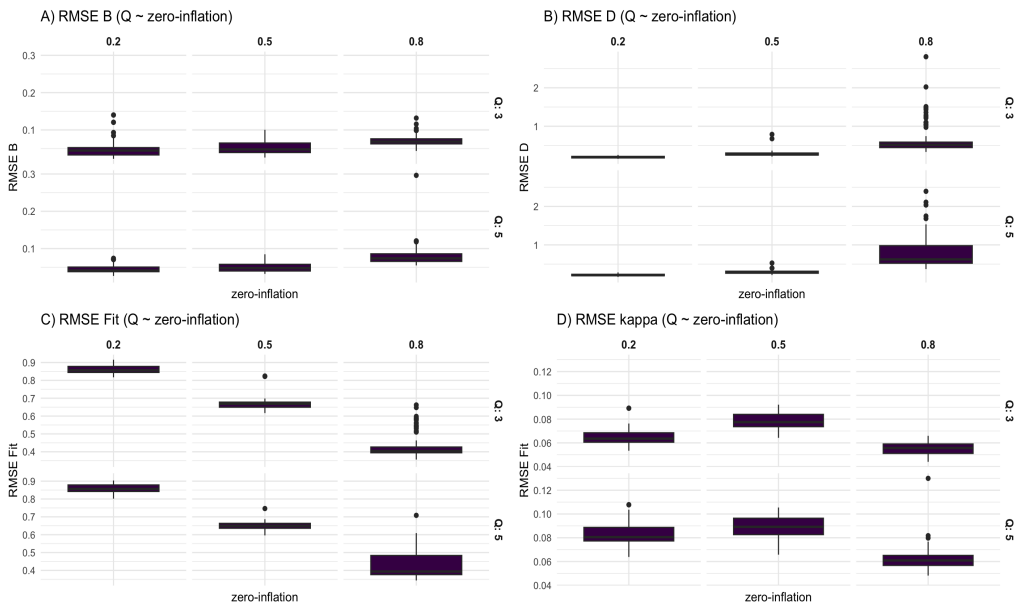


Figure 4: RMSE measured for zero-inflated data, for B (A), D (B), for real-data fitting (C) and for κ (D) for different values of Q and different zero-inflation level.

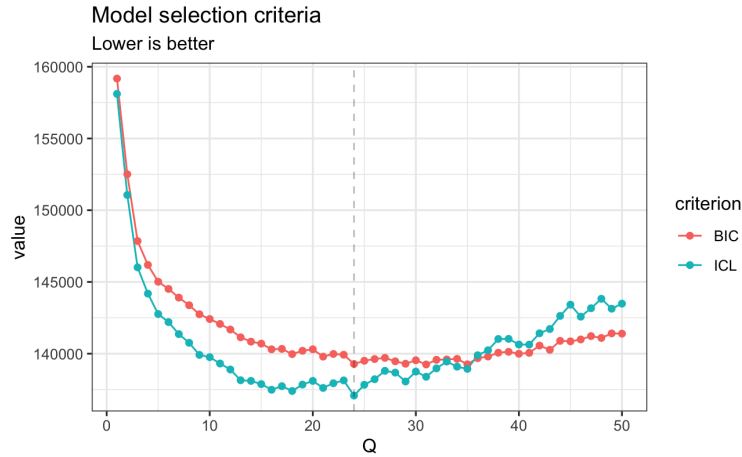


Figure 5: BIC and ICL criteria as a function of the number of clusters Q for the integrated inference method applied to the breast cancer dataset.

show how the clustering it outputs may help retrieve connections between different pathways. Then we use a regularized Normal-Block model to analyse words occurrences on webpages and how the different groups of words tend to be found together or not. Finally we use a zero-inflated regularized Normal-Block model to study animal microbiota data. Data and code for these illustrations are available in the *inst* folder of the **normalblockr** github repository.

6.1. Breast cancer proteomics data

We first use Normal-Block to analyse proteomics data of breast cancer from Brigham & Women’s Hospital & Harvard Medical School (2012) obtained with reverse-phase protein arrays. We pre-process the data to remove proteins whose expressions are highly correlated. We also remove the sites (that is, tumors here) that appear as outliers on a PCA of the proteins expressions. We consider the standardized expressions of $p = 163$ proteins in $n = 346$ tumors. We use the breast cancer subtypes as covariates (Normal-Like, Basal, Luminal A, Luminal B and HER2-enriched) and run the integrated inference from $Q = 1$ to $Q = 50$ clusters. Using the ICL, we fix $Q = 24$ clusters (Figure 5).

We then run an enrichment analysis based on the Kyoto Encyclopedia of Genes and Genomes (KEGG) on the resulting clusters with a p-value threshold of 0.001, using R packages **cluster-Profiler** and **enrichplot** (Yu et al. , 2012; Yu and Gao , 2025). The results are shown on Figure 6. 10 clusters out of 24 display distinct enrichment patterns that pass the p-value threshold. Some of the pathway combinations appear meaningful from a biological point of view. For instance, PI3K-Akt and focal adhesion pathways are identified together in cluster 3 and they happen to be related in certain cancer cells (Matsuoka et al., 2012). Another example is the identification of both EGFR and mTOR pathways in clusters 6 and 13, in breast cancers, the overexpression of EGFR is associated with the activation of the PI3K/Akt/mTOR pathway (El-Guerrab et al., 2020)

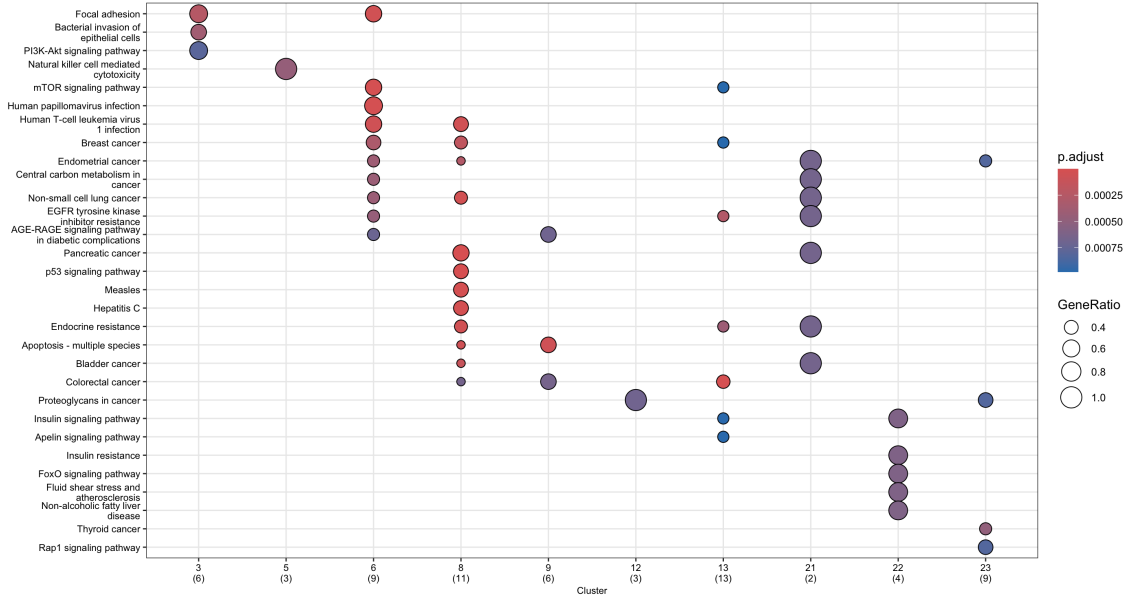


Figure 6: Enrichment plot for the clusters obtained with Normal-Block. Below the cluster labels is given the number of genes from the cluster that is associated with one of the identified pathways.

6.2. University webpages

Following Tan et al. (2015)’s illustration for their cluster Graphical-Lasso, we use Normal-Block for words frequencies analysis on webpages from the ”4 universities data set” accessible on www.cs.cmu.edu. This dataset from the ”World Wide Knowledge Base” project at Carnegie Mellon University gathers web pages from four universities: Cornell, Texas, Washington, and Wisconsin. We process the data as indicated in Tan et al. (2015) but they used pre-processed data Cardoso-Cachopo (2009) that we could not have access to.

We consider students webpages only, leaving us with $n = 504$ pages and $p = 1867$ words after removal of stop words and of words occurring only once in the whole dataset.

Let f_{ij} be the frequency of the j -th word on the i -th page. We consider $\tilde{Y} \in \mathbb{R}^{n \times p}$ defined by $Y_{ij} = \log(1 + f_{ij})$. We only keep the $p = 100$ words with maximal entropy, with entropy for the j -th term defined as $-\sum_{i=1}^n g_{ij} \log(g_{ij}) / \log(n)$ with $g_{ij} = \frac{f_{ij}}{\sum_{i=1}^n f_{ij}}$. We then obtain Y from \tilde{Y} standardizing each column to have mean 0 and standard deviation 1. We run the model with $Q = 15$ clusters and a sparsity penalty $\lambda = 0.005$. The clustering is described in table 6.2 and the network is shown on Figure 7.

As in Tan et al. (2015), we see that words like ”office”, ”phone” and ”email” or ”student” and ”graduate” tend to be grouped together so that our clustering seems consistent with the one they obtain. Other groupings are meaningful such as that of ”conference”, ”workshop” and ”paper” in cluster 3, ”parallel” and ”programming” in cluster 10 or ”austin” and ”texas” in cluster 15.

In the network we see on the one hand that the group of generic ”administrative” words represented by cluster 9 tend not to be found with other more computer-science related words in cluster 15. On the other hand, clusters 8 and 3 display a positive association, maybe because

cluster	words
1	research, thu, data, performance
2	postscript, available, game
3	systems, system, proceedings, distributed, report, operating, conference, workshop, paper
4	seattle, class, summer
5	work, project
6	also, software, like, web, stuff, date, david
7	madison, wisconsin, sep, usa, really
8	appear, international, james
9	home, page, office, phone, email, number
10	parallel, programming, group
11	interests, theory, one, compiler, language, think, design, languages
12	department, time, cornell, homepage, seed
13	nov, can, monday, student, graduate, engineering, working, wednesday, links, oct, jan, currently, may, current, new, school, fall, will, see, java, first, year, interesting, server, database, algorithms
14	people, computers, two, well, make, program
15	computer, university, austin, science, information, texas, address, sciences, using, learning

Table 2: List of Words by cluster in the "4 universities dataset"

they both relate to scientific communication.

6.3. Microbiota members from dairy cows

We consider a dataset produced with the MICROCOSM project by INRAE (Mariadassou et al., 2023), the data are derived from sequence data available in the Sequence Read Archive of the National Center for Biotechnology Information under the accession number PRJNA 875059 and processed as detailed in doi:10.1186/s42523-023-00252-w.. It consists of microbiota from the mouth, nose, vagina and milk of 45 lactating dairy cows, collected at 4 time points during their first lactation, from 1-week pre-partum to 7-month post-partum. We obtain a count matrix of dimensions $n = 899$ (number of (*site, sampling moment, cow*)), $p = 259$ Amplicon Sequence Variants (ASVs) that we log-transform.

As the dataset contains a lot of zeros, we use the zero-inflated Normal-Block model, with the integrated inference procedure. Figure 8 shows a good fit quality of the model. We compare several initial clustering, based on the residuals and zero-inflation posterior probabilities of a diagonal zero-inflated normal model. We fix $Q = 5$ and add sparsity in the model. A comparison with taxonomy at different levels (Phylum, Class, Order, Family, Genus, Species) based on the ARI shows that the inferred clustering catches a little bit of the taxonomy at the Order level (Table 3). More importantly, we consider a clustering based on the posterior probability of zero-inflation (ρ with our notations) using hierarchical clustering of variables, with R package **ClustOfVar**. The results show that most of the taxonomy signal is actually contained in the zero-inflation patterns (Table 3). Figure 9 underlines this, showing distinct patterns of zero-inflation from one ASV cluster to another. The model's network is shown on Figure 10. The results (Figure 10) show that Cluster 1 contains the most taxa and makes up for more than 80%

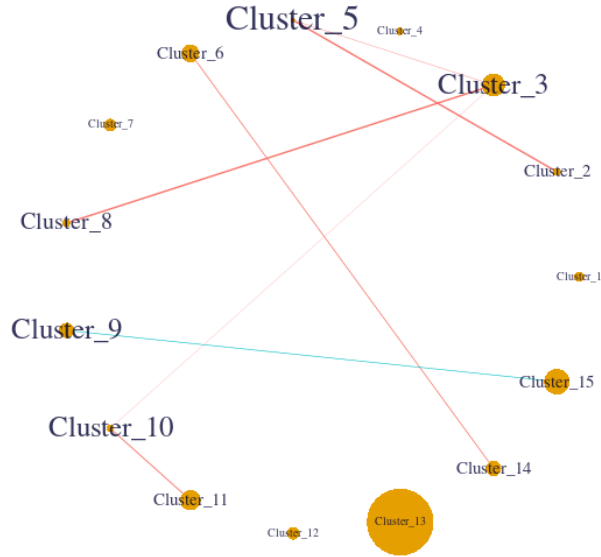


Figure 7: Network obtained with Normal-Block for the "4 universities dataset". Pink edges correspond to positive associations whereas blue edges are for negative associations, the thicker an edge, the stronger the corresponding association.

of the microbiota in almost all samples. Clusters 4 and 5 are two clusters made mainly of lactic acid bacteria (*Lactobacillus*, *Pediococcus*, *Leuconostoc*) or acid-tolerant bacteria (*Acetobacter*). Those two clusters are jointly abundant only in oral and nasal samples.

Taxonomy level	Normal-block clustering	Zero-inflation clustering (from Normal-Block)
Phylum	-0.03	0.22
Class	0.05	0.37
Order	0.06	0.41
Family	0.02	0.17
Genus	0.003	0.05
Species	0.012	0.25

Table 3: ARI results for the zero-inflated Normal-Block clustering and for the clustering inferred with hierarchical clustering of variable on the variational posterior zero-inflation probabilities for different levels of taxonomy, with 10 groups.

7. Discussion

We propose Normal-Block, a Gaussian graphical model that integrates a clustering on the variables. This adds structure to the model. Moreover, considering a network at cluster level reduces the network's dimensionality. We prove the model's identifiability when the clustering is observed and propose an inference procedure that resorts to Graphical-Lasso and uses variational expectation-maximization to simultaneously retrieve the clustering and the cluster-level-network.

A limitation of Graphical-Lasso and other penalized methods for network inference lies in the lack of structure they assume, as well as the complexity associated with network inference

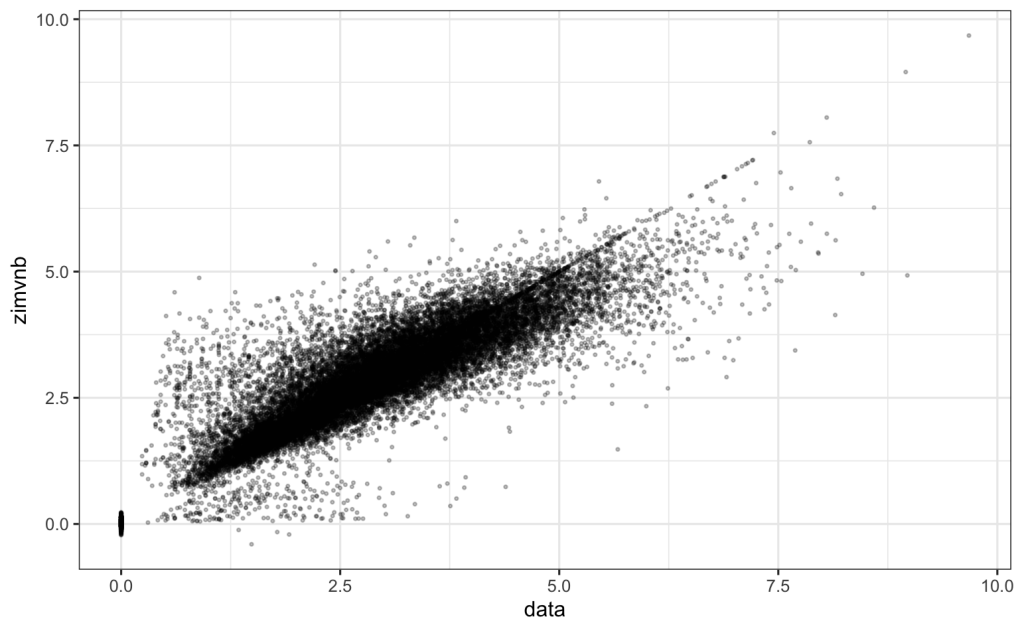


Figure 8: Fitted MICROCOSM data with sparse zero-inflate Normal-Block model with 10 groups as a function of real MICROCOSM data.

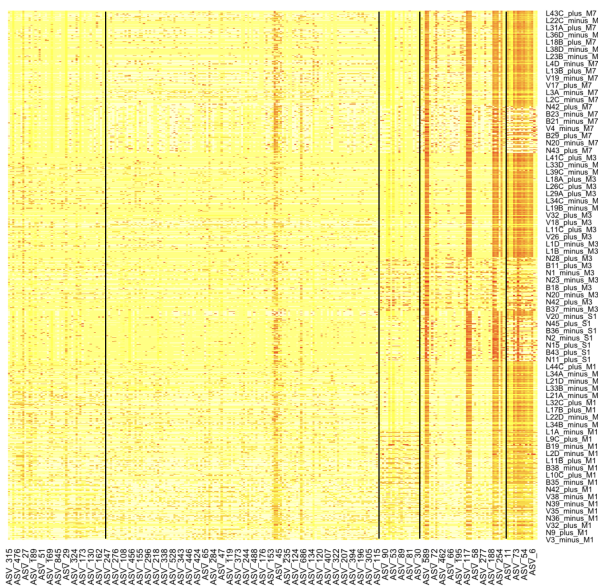


Figure 9: Heatmap of the variational posterior zero-inflation probabilities (ρ) sorted by clusters inferred with hierarchical clustering of variables. Black lines delimit clusters.

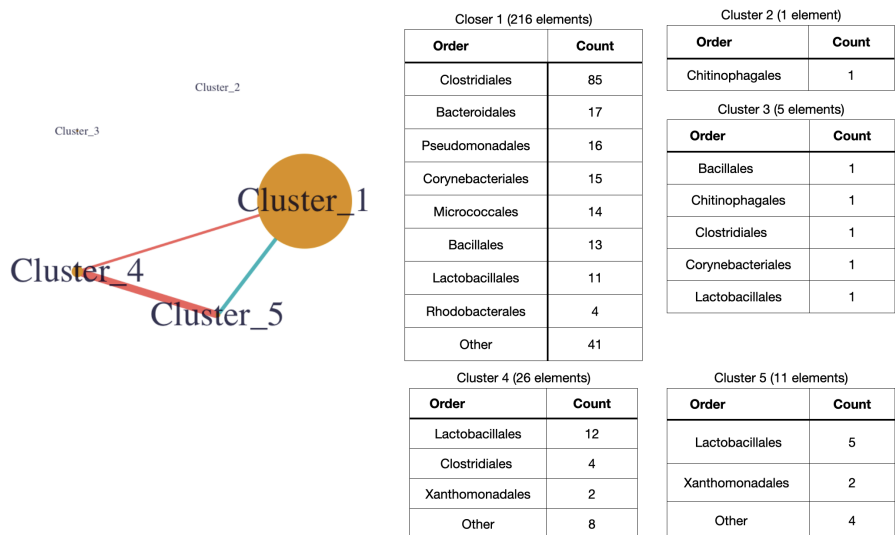


Figure 10: Network obtained for the Microcosm data with a sparse zero-inflated Normal-Block model, and the main taxonomic groups represented in each cluster.

and interpretation as its dimension grows. The Normal-Block adds a structure hypothesis on the network and builds on this hypothesis to reduce the network’s dimension.

We have shown on simulated data that both the clustering and the network inference work well, provided the zero-inflation remains limited, but we have no theoretical results on the model’s identifiability when the clustering is not observed or on the global concavity of the ELBO.

The model could further be developed to introduce other forms of zero-inflation, for instance making it individual-dependent or covariate-dependent instead of variable-dependent. It could also be useful to add other *a priori* hypotheses that would constrain the network structure, for instance forbidding or favouring specific associations to appear in the network. Finally, several temporal extensions of the model could be designed, to consider a clustering or a network that could evolve at each time step.

Acknowledgements

We thank Mahendra Mariadassou for his insights in the analysis of the MICROCOSM dataset. This work was partially supported by a funding of the ANR SingleStatOmics.

Appendices

A. Proofs of identifiability in the observed clusters models

A.1. Spherical model

In this model we have $Y_i \ p_\theta(Y_i) = \mathcal{N}(\mu_i = B^\top X_i, S = D + C\Sigma C^\top)$ with $D = \text{diag}(\xi), \xi \in \mathbb{R}^+$ and the model parameters $\theta = (\xi, B, \Sigma)$. Let us assume that no group is empty.

Given two sets of parameters θ, θ' , for $i \in \llbracket 1; n \rrbracket$:

$$\begin{aligned} P_\theta(Y_i) &= P_{\theta'}(Y_i) \\ \Leftrightarrow \|Y_i - \mu\|_{S^{-1}} - \log |S| &= \|Y_i - \mu'\|_{S'^{-1}} - \log |S'| \\ \Leftrightarrow Y_i^\top (S^{-1} - S'^{-1})Y_i - 2Y_i^\top (S^{-1}\mu - S'^{-1}\mu') & \\ + \mu^\top S^{-1}\mu - \mu'^\top S'^{-1}\mu' + \log |S| - \log |S'| &= 0 \end{aligned}$$

which is equal to zero when $\xi I_p + C\Sigma C^\top = \xi' I_p + C\Sigma' C^\top$ and $\mu_i = \mu'_i \Leftrightarrow (B - B')^\top X_i = 0$. Having $\forall i \in \llbracket 1; n \rrbracket, (B - B')^\top X_i = 0$ is equivalent to $(B - B')^\top X = 0$. Thus, if X is of rank d , we have $B = B'$.

For variance, we assume that no group is empty so that:

$$\begin{aligned} \forall q^*, k^* \in \llbracket 1; Q \rrbracket, q^* \neq k^*, \exists j, l \in \llbracket 1; p \rrbracket, q(j) = q^*, q(l) = k^* \\ (C\Sigma'_Q C^\top)_{jl} = \sigma'_{q^* k^*} = \sigma_{q^* q^*} \end{aligned}$$

This proves the equality between Σ_Q and Σ'_Q off-diagonal terms.

On the diagonal of S' :

$$\forall j \in \llbracket 1; p \rrbracket, S'_{jj} = \xi' + \sigma'_{q(j)q(j)} = \xi + \sigma_{q(j)q(j)}$$

Let us assume that there exists one group q^* that contains at least two elements.

$$\begin{aligned} \exists j^*, l^* \in \llbracket 1; p \rrbracket, j^* \neq l^*, q(j^*) = q(l^*) = q^* \\ (C\Sigma'_Q C^\top)_{j^* l^*} = \sigma'_{q^* q^*} = \sigma_{q^* q^*} \\ S'_{j^* j^*} = \xi' + \sigma'_{q^* q^*} \\ = \xi' + \sigma_{q^* q^*} \end{aligned}$$

Thus we have $\xi = \xi'$.

The diagonal expression $\xi' + \sigma'_{q(j)q(j)} = \xi + \sigma_{q(j)q(j)}$ finally gives us the equality between Σ_Q and Σ'_Q diagonal terms.

Therefore, the model is identifiable as long as X_i is a full-rank matrix, no cluster is empty and at least one of the clusters contains at least two elements.

A.2. General model

In this model we have $Y_i \ p_\theta(Y_i) = \mathcal{N}(\mu = B^\top X_i, S = D + C\Sigma C^\top)$ with $D = \text{diag}(d), d \in \mathbb{R}^{+p}$ and the model parameters $\theta = (d, B, \Sigma)$. Let us assume that no group is empty.

Given two sets of parameters θ, θ' :

$$\begin{aligned} P_\theta(Y_i) &= P_{\theta'}(Y_i) \\ \Leftrightarrow \|Y_i - \mu\|_{S^{-1}} - \log |S| &= \|Y_i - \mu'\|_{S'^{-1}} - \log |S'| \\ \Leftrightarrow Y_i^T (S^{-1} - S'^{-1}) Y_i - 2Y_i^T (S^{-1} \mu - S'^{-1} \mu') \\ &\quad + \mu^T S^{-1} \mu - \mu'^T S'^{-1} \mu' + \log |S| - \log |S'| = 0 \end{aligned}$$

which is equal to zero when $\xi I_p + C \Sigma C^T = \xi' I_p + C \Sigma' C^T$ and $\mu = \mu' \Leftrightarrow B^T X_i = B'^T X_i \Rightarrow B = B'$ and $X_i^T X_i$ non singular (thus full-rank X_i).

For variance, we assume that no group is empty so that:

$$\begin{aligned} \forall q^*, k^* \in \llbracket 1; Q \rrbracket, q^* \neq k^*, \exists j, l \in \llbracket 1; p \rrbracket, q(j) = q^*, q(l) = k^* \\ (C \Sigma_Q' C^T)_{jl} = \sigma'_{q^* k^*} = \sigma_{q^* q^*} \end{aligned}$$

This proves the equality between Σ_Q and Σ_Q' off-diagonal terms.

Let us also assume that each group q contains at least two elements.

$$\begin{aligned} \forall q^* \in \llbracket 1; Q \rrbracket, \exists j, l \in \llbracket 1; p \rrbracket, j \neq l, q(j) = q(l) = q^* \\ (C \Sigma_Q' C^T)_{jl} = \sigma'_{q^* q^*} = \sigma_{q^* q^*} \end{aligned}$$

This proves the equality between Σ_Q and Σ_Q' diagonal terms, provided each group contains at least two elements.

Finally on the diagonal of S'' :

$$\begin{aligned} \forall j \in \llbracket 1; p \rrbracket, S_{jj} &= d_j + \sigma'_{q(j)q(j)} \\ &= d_j + \sigma_{q(j)q(j)} \\ &= d_j + \sigma_{q(j)q(j)} \end{aligned}$$

This proves that $d'_j = d_j$. Thus, the model is identifiable provided each group contains at least two elements.

If one group q^* contains only one element j however, any $d_j + \epsilon, \epsilon > -d_j, \epsilon < \sigma_{q^* q^*}$ can give the same likelihood, replacing $\sigma_{q^* q^*}$ with $\sigma'_{q^* q^*} = \sigma_{q^* q^*} - \epsilon$.

Therefore the observed-clusters model is identifiable provided the X_i are full rank and each cluster contains at least two elements.

B. Concavity results

For the various models the concavity proofs are based on the Hessian's (denoted \mathcal{H}) computation and analysis.

B.1. observed clusters spherical model

For this model we get the first-order differential:

$$\begin{aligned} dJ &= -\frac{np}{2} \xi d\xi^{-1} - \frac{1}{2} \text{tr}(RR^T) d\xi^{-1} + \xi^{-1} \text{tr}(Y^T X dB) - \xi^{-1} \text{tr}(B^T X^T X dB) \\ &\quad + \text{tr}(RC \mu^T) d\xi^{-1} - \xi^{-1} \text{tr}(C \mu^T X dB) - \frac{n}{2} \text{tr}(C^T C \Gamma) d\xi^{-1} - \frac{1}{2} \text{tr}(\mu(C^T C) \mu^T) d\xi^{-1} \\ &\quad + \frac{n}{2} \text{tr}(\Omega_Q^{-1} d\Omega_Q) - \frac{n}{2} \text{tr}(\Gamma d\Omega_Q) - \frac{1}{2} \text{tr}(\mu^T \mu d\Omega_Q) \end{aligned}$$

and the second-order differential:

$$\begin{aligned} d^2J = & -\frac{np}{2}\xi^2 d\xi^{-1} d\xi^{-1} + 2\text{tr}(Y^\top X dB) d\xi^{-1} - 2\text{tr}(B^\top X^\top X dB) d\xi^{-1} \\ & - \xi^{-1} \text{tr}(dB^\top X^\top X dB) - 2\text{tr}(C\mu^\top X dB) d\xi^{-1} - \frac{n}{2}\text{tr}(\Omega_Q^{-1} d\Omega_Q \Omega_Q^{-1} d\Omega_Q) \end{aligned}$$

Hence the following hessian, where $\omega = \xi^{-1}$ and $R_\mu = (Y - XB - \mu C^\top)$:

$$\begin{pmatrix} \partial^2 \text{vec}(\Omega_Q) & 0 & 0 \\ \partial^2 \omega & -\frac{np}{2}\omega^{-2} & 2\text{vec}(X^\top R_\mu) \\ \partial^2 \text{vec}(B) & -\omega(I_p \otimes X^\top X) & \end{pmatrix}$$

We have $-\frac{np}{2}\omega^{-2} < 0$. Σ_Q is positive definite so that $-\frac{n}{2}\Sigma_Q \otimes \Sigma_Q$ is negative definite. $X^\top X$ is positive, it is positive definite if X is full-rank so that $-\omega(I_p \otimes X^\top X)$ is negative, and negative definite if X is full-rank, since $\omega > 0$. This proves the joint concavity of J in (Ω_Q, ξ^{-1}) and in (Ω_Q, B) .

B.2. observed clusters general model

For this model we get the first-order differential:

$$\begin{aligned} dJ = & \frac{n}{2}\text{tr}(DdD^{-1}) - \frac{1}{2}\text{tr}(RdD^{-1}R^\top) + \text{tr}(XdBD^{-1}Y^\top) - \text{tr}(D^{-1}B^\top X^\top X dB) \\ & + \text{tr}(RdD^{-1}C\mu^\top) - \text{tr}(D^{-1}C\mu^\top X dB) - \frac{n}{2}\text{tr}(C\Gamma C^\top dD^{-1}) - \frac{1}{2}\text{tr}(\mu C^\top dD^{-1}C\mu^\top) \\ & + \frac{n}{2}\text{tr}(\Sigma_Q d\Omega_Q) - \frac{n}{2}\text{tr}(d\Omega_Q \Gamma) - \frac{1}{2}\text{tr}(\mu d\Omega_Q d\mu^\top) \end{aligned}$$

and the second-order differential:

$$\begin{aligned} d^2J = & -\frac{n}{2}\text{tr}(DdD^{-1}DdD^{-1}) + 2\text{tr}(Y^\top X dB dD^{-1}) - 2\text{tr}(dD^{-1}B^\top X^\top X dB) \\ & - \text{tr}(D^{-1}dB^\top X^\top X dB) - 2\text{tr}(dD^{-1}C\mu^\top X dB) - \frac{n}{2}\text{tr}(\Sigma_Q d\Omega_Q \Sigma_Q d\Omega_Q) \end{aligned}$$

Hence the following hessian, where $R_\mu = (Y - XB - \mu C^\top)$:

$$\begin{pmatrix} \partial^2 \text{vec}(\Omega_Q) & 0 & 0 \\ \partial^2 D^{-1} & -\frac{n}{2}D \otimes D & 2\text{vec}(X^\top R_\mu) \\ \partial^2 \text{vec}(B) & -D^{-1} \otimes X^\top X & \end{pmatrix}$$

As above, since D is a diagonal matrix with strictly positive elements on the diagonal, we have that the diagonal terms are negative definite hence the concavity results.

B.3. Unobserved clusters model

We recall that:

$$\begin{aligned}
J &= -n \left(\frac{p+Q}{2} \right) \log(2\pi) + \frac{nQ}{2} \log(2\pi e) \\
&\quad - \frac{n}{2} \log(\det(D)) - \frac{1}{2} \mathbf{1}_n^\top R^2 D^{-1} \mathbf{1}_p - \frac{1}{2} \mathbf{1}_n^\top M^2 \tau^\top D^{-1} \mathbf{1}_p - \frac{1}{2} \mathbf{1}_n^\top S \tau^\top D^{-1} \mathbf{1}_p \\
&\quad + \mathbf{1}_n^\top (R \odot M \tau^\top) D^{-1} \mathbf{1}_p \\
&\quad + \frac{n}{2} \log \det(\Omega_Q) - \frac{1}{2} \mathbf{1}_n^\top (M \Omega_Q \odot M) \mathbf{1}_Q - \frac{1}{2} \mathbf{1}_n^\top S \text{diag}(\Omega_Q) + \frac{1}{2} \mathbf{1}_n^\top \log(S) \mathbf{1}_Q \\
&\quad + \mathbf{1}_p^\top \tau \log(\alpha) - \mathbf{1}_p^\top ((\tau \odot \log(\tau))) \mathbf{1}_Q
\end{aligned}$$

B.3.1. Concavity in B

Let us consider only the terms of J whose double derivation in B is non-zero:

$$\begin{aligned}
\tilde{J}(B) &= -\frac{1}{2} \mathbf{1}_n^\top R^2 D^{-1} \\
\partial_{B,B}^2 J &= -\frac{n}{2} \text{tr}(D^{-1} dB^\top X^\top X dB) \\
\mathcal{H}_{B,B} &= -D^{-1} \otimes (X^\top X)
\end{aligned}$$

D^{-1} is a diagonal matrix with positive elements only, $X^\top X$ is always a positive matrix, and is definite positive if X has full rank. Thus, $\mathcal{H}_{B,B}$ is a negative matrix, and J is concave in B.

B.3.2. Concavity in D^{-1}

Let us consider only the terms of J whose double derivation in D^{-1} is non-zero:

$$\begin{aligned}
\tilde{J}(D^{-1}) &= -\frac{n}{2} \log(\det(D)) \\
\partial_{D^{-1}, D^{-1}}^2 J &= -\frac{n}{2} \text{tr}(D dD^{-1} D dD^{-1}) \\
\mathcal{H}_{D^{-1}, D^{-1}} &= -\frac{n}{2} D \otimes D
\end{aligned}$$

D^{-1} is a diagonal matrix with positive elements only so that $\mathcal{H}_{D^{-1}, D^{-1}}$ is negative definite and J is concave in D^{-1}

B.3.3. Concavity in Ω_Q

Let us consider only the terms of J whose double derivation in Ω_Q is non-zero:

$$\begin{aligned}
\tilde{J}(\Omega_Q) &= \frac{n}{2} \log(\det(\Omega_Q)) \\
\partial_{\Omega_Q, \Omega_Q}^2 J &= -\frac{n}{2} \text{tr}(\Sigma_Q d\Omega_Q \Sigma_Q d\Omega_Q) \\
\mathcal{H}_{\Omega_Q, \Omega_Q} &= -\frac{n}{2} \Sigma_Q \otimes \Sigma_Q
\end{aligned}$$

Σ_Q is a positive definite matrix so that only so that $\mathcal{H}_{\Omega_Q, \Omega_Q}$ is negative definite and J is concave in Ω_Q

B.3.4. Concavity in α

We can compute it "by hand" since α is a vector.

$$\begin{aligned}\tilde{J}(\alpha) &= \mathbf{1}_p^\top \tau \log(\alpha) \\ \frac{\partial J}{\partial \alpha_q} &= \frac{\sum_{j=1}^p \tau_{jq}}{\alpha_q}\end{aligned}$$

$\mathcal{H}_{\alpha,\alpha}$ is a matrix of dimensions Q, Q whose term (k, q) is equal to $\frac{\partial J}{\partial \alpha_k \partial \alpha_q}$, which is equal to 0 if $k \neq q$ and to $-\frac{\sum_{j=1}^p \tau_{jq}}{\alpha_q^2}$ otherwise.

B.3.5. Concavity in M

Let us consider only the terms of J whose double derivation in M is non-zero:

$$\begin{aligned}\tilde{J}(M) &= -\frac{1}{\mathbf{1}_n} M^2 \tau^\top D^{-1} \mathbf{1}_p - \frac{1}{2} \mathbf{1}_n^\top (M \Omega_Q \odot M) \mathbf{1}_Q \\ &= -\frac{1}{2} \sum_{i,j} \sum_{q=1}^Q \tau_{jq} M_{iq}^2 D_{jj}^{-1} - \frac{1}{2} \sum_{i=1}^n \sum_{k,q=1}^Q M_{ik} M_{iq} \Omega_{Q_{kq}} \\ \frac{\partial \tilde{J}}{\partial M_{iq}} &= -\sum_{j=1}^p \tau_{jq} D_{jj}^{-1} M_{iq} - \sum_{k=1,k \neq q}^Q M_{ik} \Omega_{Q_{kq}} \\ \frac{\partial^2 \tilde{J}}{\partial^2 M_{iq}} &= -\sum_{j=1}^p \tau_{jq} D_{jj}^{-1} - \Omega_{Q_{qq}} \\ \frac{\partial^2 \tilde{J}}{\partial M_{iq} \partial M_{iq_2}} &= -\Omega_{Q_{kq}} \text{ if } q \neq q_2 \\ \frac{\partial^2 \tilde{J}}{\partial M_{iq} \partial M_{i_2 q_2}} &= 0 \text{ if } i \neq i_2 \text{ and } q \neq q_2 \\ \mathcal{H}_{M,M} &= -I_n \otimes (\text{diag}(\tau^\top D^{-1} \mathbf{1}_p) - \Omega_Q)\end{aligned}$$

τ only contains positive values and so does the diagonal of D^{-1} so that $\tau^\top D^{-1} \mathbf{1}_p$ is positive definite and so is Ω_Q . Finally $\mathcal{H}_{M,M} = -I_n \otimes (\text{diag}(\tau^\top D^{-1} \mathbf{1}_p) - \Omega_Q)$ is negative definite, we get the concavity in M .

B.3.6. Concavity in S

Considering only terms whose double derivation in S is not equal to 0:

$$\begin{aligned}\tilde{J}(S) &= \frac{1}{2} \sum_{i,q} \log(S_{iq}) \\ \frac{\partial \tilde{J}}{\partial S_{iq}} &= \frac{1}{2} \frac{1}{S_{iq}} \\ \frac{\partial^2 \tilde{J}}{\partial^2 S_{iq}} &= -\frac{1}{2} \frac{1}{S_{iq}^2} \\ \frac{\partial^2 \tilde{J}}{\partial S_{iq} \partial S_{i_2 q_2}} &= 0 \text{ if } i \neq i_2 \text{ or } q \neq q_2 \\ \mathcal{H}_{S,S} &= -\frac{1}{2} \text{diag} \left(\text{vec} \left(\frac{1}{S^2} \right) \right)\end{aligned}$$

B.3.7. Concavity in τ

Considering only terms whose double derivation wrt τ is not equal to 0:

$$\begin{aligned}\tilde{J}(\tau) &= -\mathbf{1}_p^\top (\tau \odot \log(\tau)) \mathbf{1}_Q \\ &= \sum_{j,q} \tau_{jq} \log(\tau_{jq}) \\ \frac{\partial \tilde{J}}{\partial \tau_{jq}} &= -\log(\tau_{jq}) - 1 \\ \frac{\partial^2 \tilde{J}}{\partial^2 \tau_{jq}} &= -\frac{1}{\tau_{jq}} \\ \frac{\partial^2 \tilde{J}}{\partial \tau_{jq} \partial \tau_{j_2 q_2}} &= 0 \text{ if } j \neq j_2 \text{ or } q \neq q_2 \\ \mathcal{H}_{\tau,\tau} &= -\text{diag} \left(\text{vec} \left(\frac{1}{\tau} \right) \right)\end{aligned}$$

which is negative definite because τ only contains positive values.

C. ELBO and estimators for the zero-inflated model

For the zero-inflated Normal-Block, we obtain the following ELBO:

$$\begin{aligned}J &= \overline{P \circ \delta_{0,\infty}(Y)} - \frac{1}{2} \mathbf{1}_n^\top \left(Q \circ (AD^{-1} + \mathbf{1}_n \otimes \log(d) + \log(2\pi)) \right) \mathbf{1}_p \\ &\quad - \frac{nK}{2} \log(2\pi) - \frac{1}{2} \text{tr} \left(\Omega_K (n\Gamma + \mu\mu^\top) \right) - \frac{n}{2} \log |\Sigma_Q| \\ &\quad + \mathbf{1}_n^\top (P \log(\pi) + Q \log(1 - \pi)) \\ &\quad - \overline{P \log(P)} - \overline{Q \log(Q)} + \frac{nK}{2} \log(2\pi e) + \frac{1}{2} \overline{\log(S)} \\ &\text{with: } R = Y - XB, P = (\rho_{ij}), Q = 1 - P, \text{ and } A = (R - MC^\top)^2 + SC^\top\end{aligned}$$

The VE-step then consists in updating M, S and $(\rho_{ij})_{ij}$. We have explicit estimators for S and $(\rho_{ij})_{ij}$ but not for M , for which we resort to numerical optimization using a gradient ascent. For the M-step, we update D and Ω_Q with explicit estimators and estimate B through gradient ascent (Proposition C.1).

Proposition C.1. *For the zero-inflated observed-clusters model, explicit estimators are given for $S, P = (\rho_{ij})_{ij}, d, \kappa$ and Ω_Q by:*

$$\begin{aligned}\hat{S} &= \left(QD^{-1}C + \mathbf{1}_n \otimes \text{diag}(\Omega_K) \right)^\circ, \quad P = \mathbb{1}_{\{Y=0\}} \circ \frac{\exp(v)}{1 + \exp v}, \quad \hat{d} = \overline{(Q \circ A)} / \overline{Q}, \\ \hat{\kappa} &= \frac{1}{n} \overline{P}, \quad \hat{\Sigma}_Q = \frac{1}{n} (M^T M + \text{Diag}(\overline{S})),\end{aligned}$$

denoting $v = \frac{1}{2}(AD^{-1} + \mathbf{1}_n \otimes \log(d) + \log(2\pi)) + \mathbf{1}_n \otimes \log\left(\frac{\pi}{1-\pi}\right)$.

We get M by maximizing $F(M) = -\frac{1}{2} \mathbf{1}_n^T (QD^{-1} \circ (R - MC^T)^2) \mathbf{1}_p - \frac{1}{2} \text{tr}(\Omega_K M^T M)$ with $\nabla_M F(M) = (QD^{-1} \circ (R - MC^T))C - M\Omega_K$.

\hat{B} is estimated by maximizing $F(B) = -\frac{1}{2} \mathbf{1}_n^T (QD^{-1} \circ (R - MC^T)^2) \mathbf{1}_p$ with $\nabla_B F(B) = X^T (QD^{-1} \circ (R - MC^T))$

When the clustering is unobserved, we also use a variational approximation, similarly to what we have previously done. The ELBO becomes:

$$\begin{aligned}J &= \overline{P \circ \delta_{0,\infty}(Y)} - \frac{1}{2} \mathbf{1}_n^T (Q \circ (AD^{-1} + \mathbf{1}_n \otimes \log(d) + \log(2\pi))) \mathbf{1}_p, \\ &+ \mathbf{1}_n^T (P \log(\pi) + Q \log(1 - \pi)) + \overline{\tau \log(\alpha)}, \\ &- \frac{nK}{2} \log(2\pi) - \frac{1}{2} \text{tr}(\Omega_K (\text{Diag}(\overline{S}) + M^T M)) - \frac{n}{2} \log |\Sigma_Q|, \\ &- \overline{\tau \circ \log(\tau)} - \overline{P \log(P)} - \overline{Q \log(Q)} + \frac{nK}{2} \log(2\pi e) + \frac{1}{2} \overline{\log(S)},\end{aligned}$$

with: $R = Y - XB, P = (\rho_{ij})_{ij}, Q = 1 - P, A = R^2 - 2R \circ M\tau^T + (M^2 + S)\tau^T$

We proceed in the same way for the VE and M steps, having explicit estimators for $S, (\rho_{ij})_{ij}, D, \Omega_Q$ but not for M and B for which we use a gradient ascent approach (see Proposition C.2).

Proposition C.2. *For the zero-inflated unobserved-clusters model, explicit estimators are given for $S, P = (\rho_{ij})_{ij}, \tau, d, \kappa, \Omega_Q$ and α by:*

$$\begin{aligned}\hat{S} &= \left(QD^{-1}\tau + \mathbf{1}_n \otimes \text{diag}(\Omega_K) \right)^\circ, \quad \hat{P} = \mathbb{1}_{\{Y=0\}} \circ \frac{\exp(v)}{1 + \exp v}, \quad \hat{\tau}_j = \text{softmax}(\eta_j), \\ \hat{d} &= \overline{(Q \circ A)} / \overline{Q}, \quad \hat{\kappa} = \frac{1}{n} \overline{P}, \quad \hat{\alpha} = \frac{1}{n} \overline{\tau}, \quad \hat{\Sigma}_Q = \frac{1}{n} (M^T M + \text{Diag}(\overline{S})),\end{aligned}$$

denoting $v = \frac{1}{2}(AD^{-1} + \mathbf{1}_n \otimes \log(d) + \log(2\pi)) + \mathbf{1}_n \otimes \log\left(\frac{\pi}{1-\pi}\right)$ and $\eta = -\frac{1}{2}(QD^{-1})^T (M^2 + S) + (QD^{-1} \circ R)^T M + \mathbf{1}_p \otimes \log(\alpha) - 1$

We get M by maximizing $F(M) = -\frac{1}{2} \mathbf{1}_n^T (QD^{-1} \circ (-2R \circ M\tau^T + M^2\tau^T)) \mathbf{1}_p - \frac{1}{2} \text{tr}(\Omega_K M^T M)$ with $\nabla_M F(M) = (QD^{-1} \circ R)\tau - QD^{-1}\tau \circ M - M\Omega_K$.

\hat{B} is estimated by maximizing $F(B) = -\frac{1}{2} \mathbf{1}_n^T (QD^{-1} \circ (R^2 - 2R \circ M\tau^T)) \mathbf{1}_p$ with $\nabla_B F(B) = X^T (QD^{-1} \circ (R - M\tau^T))$.

References

- The 4 universities data set, 1998, <https://www.cs.cmu.edu/afs/cs/project/theo-20/www/data/> [Consulted on: February 5th, 2025].
- Elizabeth S. Allman, Catherine Matias, and John A. Rhodes, *Identifiability of parameters in latent structure models with many observed variables*, 2009.
- Elizabeth S. Allman, Catherine Matias, and John A. Rhodes, *Parameter identifiability in a class of random graph mixture models*, *Journal of Statistical Planning and Inference*, 141(5), 1719–1736, 2011.
- Christophe Ambroise, Julien Chiquet, and Catherine Matias, *Inferring sparse Gaussian graphical models with latent structure*, 2009.
- Onureena Banerjee, Laurent El Ghaoui, and Alexandre d’Aspremont, *Model selection through sparse maximum likelihood estimation for multivariate Gaussian or binary data*, *The Journal of Machine Learning Research*, 9, 485–516, 2008.
- Bastien Batardière, Julien Chiquet, François Gindraud, and Mahendra Mariadassou, *Zero-inflation in the Multivariate Poisson Lognormal Family*, arXiv preprint arXiv:2405.14711, 2024.
- Eugene Belilovsky, Kyle Kastner, Gaël Varoquaux, and Matthew B. Blaschko, *Learning to discover sparse graphical models*, In International Conference on Machine Learning, 440–448, 2017.
- Christophe Biernacki, Gilles Celeux, and Gérard Govaert, *Assessing a mixture model for clustering with the integrated completed likelihood*, *IEEE Transactions on Pattern Analysis and Machine Intelligence*, 22(7), 719–725, 2000.
- David M. Blei, Alp Kucukelbir, and Jon D. McAuliffe, *Variational inference: A review for statisticians*, *Journal of the American Statistical Association*, 112(518), 859–877, 2017.
- Denny Borsboom, Marie K. Deserno, Mijke Rhemtulla, Sacha Epskamp, Eiko I. Fried, Richard J. McNally, Donald J. Robinaugh, Marco Perugini, Jonas Dalege, Giulio Costantini, and others, *Network analysis of multivariate data in psychological science*, *Nature Reviews Methods Primers*, 1(1), 58, 2021.
- Brigham and Women’s Hospital, Harvard Medical School, Chin Lynda, Park Peter J., Kucherlapati Raju, et al. *Comprehensive molecular portraits of human breast tumours*. *Nature* 490.7418: 61-70, 2012.
- A. Cardoso-Cachopo, *The 4 universities data set*, 2009. <http://web.ist.utl.pt/acardoso/datasets/>.
- Marie Chavent, Vabessa Kuentz, Benoit Liquet, and Jérôme Saracco, *Classification de variables: le package clustofvar*, 43èmes Journées de Statistique (SFds), 2011.
- Jiahua Chen and Zehua Chen, *Extended Bayesian information criteria for model selection with large model spaces*. *Biometrika* 95.3 (2008): 759-771.
- Khai Xiang Chiong and Hyungsik Roger Moon, *Estimation of graphical models using the L1, 2 norm*, *The Econometrics Journal*, 21(3), 247–263, 2018.
- J. Chiquet, M. Mariadassou, and S. Robin, *Variational Inference of Sparse Network from Count Data*, *Proceedings of Machine Learning Research*, 97, 1162–1171, 2019.
- J. Chiquet, S. Donnet and P. Barbillon, *sbm: Stochastic Blockmodels*, <https://CRAN.R-project.org/package=sbm>
- G. Csardi and T. Nepusz, *The igraph software*, *Complex Systems*, volume 1695, pages 1–9, 2006.
- J-J Daudin, Franck Picard, and Stéphane Robin, *A mixture model for random graphs*, *Statistics and Computing*, 18(2), 173–183, 2008.
- Arthur P. Dempster, Nan M. Laird, and Donald B. Rubin, *Maximum likelihood from incomplete data via the EM algorithm*, *Journal of the Royal Statistical Society: Series B (Methodological)*, 39(1), 1–22, 1977.
- Kevin Drew, Christian L. Müller, Richard Bonneau, and Edward M. Marcotte, *Identifying direct contacts between protein complex subunits from their conditional dependence in proteomics datasets*, *PLoS Computational Biology*, 13(10), e1005625, 2017.
- Mathias Drton and Michael D. Perlman, *Multiple testing and error control in Gaussian graphical model selection*, 2007.
- A. El Guerrab, M. Bamdad, Y. J. Bignon, F. Penault-Llorca, C. Aubeil *Co-targeting EGFR and mTOR with gefitinib and everolimus in triple-negative breast cancer cells*. *Scientific reports*, 10(1), 6367, 2020.
- Mark WEJ Fiers, Liesbeth Minnoye, Sara Aibar, Carmen Bravo González-Blas, Zeynep Kalender Atak, and Stein Aerts, *Mapping gene regulatory networks from single-cell omics data*, *Briefings in Functional Genomics*, 17(4), 246–254, 2018.
- Jerome Friedman, Trevor Hastie, and Robert Tibshirani, *Sparse inverse covariance estimation with the Graphical-Lasso*, *Biostatistics*, 9(3), 432–441, 2008.
- Jerome Friedman, Trevor Hastie, Rob Tibshirani, and Rob Tibshirani (Maintainer), *Package ‘glasso’*, 2015.
- Anne Gégout-Petit, Aurélie Muller-Gueudin, and Clémence Karmann, *Graph estimation for Gaussian data zero-inflated by double truncation*, 2019.
- Maxim Grechkin, Maryam Fazel, Daniela Witten, and Su-In Lee, *Pathway Graphical-Lasso*, *Proceedings of the AAAI Conference on Artificial Intelligence*, 29(1), 2015.
- David J. Harris, *Inferring species interactions from co-occurrence data with Markov networks*, *Ecology*, 97(12), 3308–3314, 2016.

- T. Hocking, Jean-Philippe Vert, F. Bach, and Armand Joulin, *Clusterpath: An Algorithm for Clustering Using Convex Fusion Penalties* ICMML.
- P. W. Holland, K. B. Laskey, and S. Leinhardt, *Stochastic blockmodels: First steps*, *Social Networks*, 5, 109–137, 1983.
- Daphne Koller, Nir Friedman, Lise Getoor, and Ben Taskar, *Graphical models in a nutshell*, 2007.
- Matthew K. Lau, Stuart R. Borrett, Benjamin Baiser, Nicholas J. Gotelli, and Aaron M. Ellison, *Ecological network metrics: opportunities for synthesis*, *Ecosphere*, volume 8, number 8, pages e01900, Wiley Online Library, 2017.
- Frédéric Launay, Laurent X. Nouvel, Fabienne Constant, Diego P. Morgavi, Lucie Rault, Sarah Barbey, Emmanuelle Helloin, Olivier Rué, Sophie Schbath, and others, *Microbiota members from body sites of dairy cows are largely shared within individual hosts throughout lactation but sharing is limited in the herd*, *Animal Microbiome*, 5(1), 32, 2023.
- Steffen L. Lauritzen, *Graphical models*, Clarendon Press, 1996.
- Faming Liand and Bochao Hia, *Sparse Graphical Modeling for High Dimensional Data: A Paradigm of Conditional Independence Tests*, Chapman and Hall/CRC, 2023.
- F. Lindsten, H. Ohlsson, and L. Ljung, *Clustering Using Sum-of-Norms Regularization: With Application to Particle Filter Output Computation*. IEEE Statistical Signal Processing Workshop (SSP), 201–4.
- Camilla Lingjærde, Tonje G. Lien, Ørnulf Borgan, Helga Bergholtz, and Ingrid K. Glad, *Tailored Graphical-Lasso for data integration in gene network reconstruction*, *BMC bioinformatics*, volume 22, pages 1–22, 2021, Springer.
- Han Liu, Kathryn Roeder, and Larry Wasserman, *Stability approach to regularization selection (stars) for high dimensional graphical models*, *Advances in neural information processing systems*, volume 23, 2010.
- Mark Loftus, Sayf Al-Deen Hassouneh, and Shibu Yooseph, *Bacterial associations in the healthy human gut microbiome across populations*, *Scientific reports*, volume 11, number 1, page 2828, 2021, Nature Publishing Group UK, London.
- M. Mariadassou, L. X. Nouvel, F. Constant, D. P. Morgavi, L. Rault, S. Barbey, E. Helloin, O. Rué, S. Schbath, F. Launay, and others, *Microbiota members from body sites of dairy cows are largely shared within individual hosts throughout lactation but sharing is limited in the herd*, *Animal Microbiome*, volume 5, number 1, page 32, 2023.
- Mahendra Mariadassou, Stéphane Robin, and Corinne Vacher, *Uncovering latent structure in valued graphs: a variational approach*, 2010.
- José A. Marin, Nancy K. H. Y. Lee, and James W. MacDonald, *Sparse Gaussian graphical model selection with shrinkage priors*, *Biostatistics*, 17(2), 269–281, 2016.
- Catherine Matias and Vincent Miele, *Statistical clustering of temporal networks through a dynamic stochastic block model*, *Journal of the Royal Statistical Society Series B: Statistical Methodology*, Volume 79, Issue 4, Pages 1119–1141, Oxford University Press, 2017.
- T. Matsuoka., M. Yashiro, N. Nishioka, K. Hirakawa, K., K. Olden, J.D. Roberts, J. D. , *PI3K/Akt signalling is required for the attachment and spreading, and growth in vivo of metastatic scirrhous gastric carcinoma.*, *British journal of cancer*, 106(9), Pages 1535-1542, 2012.
- Brian Matthews, Alexander R. Brown, and David R. White, *Improving Graphical-Lasso in applications to data from systems biology and gene expression studies*, *Methods*, 148, 121–130, 2018.
- Rahul Mazumder and Trevor Hastie, *The Graphical-Lasso: New insights and alternatives*, *Electronic Journal of Statistics*, volume 6, pages 2125, NIH Public Access, 2012.
- Keith McDonald, Mark J. L. McDonald, and David I. Wessels, *Eliminating dependencies among biological networks in the presence of missing data*, *Bioinformatics*, 33(11), 1783–1790, 2017.
- Nicolai Meinshausen and Peter Bühlmann, *High-dimensional graphs and variable selection with the lasso*, 2006.
- William Miller, Sarah Robinson, and David Forster, *Graphical model for network analysis in computational neuroscience*, *NeuroImage*, 202, 116072, 2019.
- Victoria Moignard, Steven Woodhouse, Laleh Haghverdi, Andrew J Lilly, Yosuke Tanaka, Adam C Wilkinson, Florian Buettner, Iain C Macaulay, Wajid Jawaid, Evangelia Diamanti, and others, *Decoding the regulatory network of early blood development from single-cell gene expression measurements*, *Nature biotechnology*, volume 33, number 3, pages 269–276, 2015, Nature Publishing Group US New York.
- Marc Ohlmann, Florent Mazel, Loïc Chalmandrier, Stéphane Bec, Eric Coissac, Ludovic Gielly, Johan Pansu, Vincent Schilling, Pierre Taberlet, Lucie Zinger, and others, *Mapping the imprint of biotic interactions on β -diversity*, *Ecology Letters*, volume 21, number 11, pages 1660–1669, 2018, Wiley Online Library.
- Kristiaan Pelckmans, Joseph De Brabanter, Johan AK Suykens, and Bart De Moor. *Convex Clustering Shrinkage.*, PAS-CAL Workshop on Statistics and Optimization of Clustering Workshop
- G. Poggiato, T. Münkemüller, D. Bystrova, J. Arbel, J.S. Clark, and W. Thuiller, *On the Interpretations of Joint Modeling in Community Ecology*, *Trends in Ecology and Evolution*, volume 2806, DOI: 10.1016/j.tree.2021.01.002, 2021.
- L.J. Pollock, R. Tingley, W.K. Morris, N. Golding, R.B. O’Hara, K.M. Parris, P.A. Vesk, and M.A. McCarthy, *Understanding co-occurrence by modelling species simultaneously with a Joint Species Distribution Model (JSDM)*, *Methods in Ecology and Evolution*, volume 5, number 5, pages 397–406, Wiley Online Library, 2014.
- Pradeep Ravikumar, Martin J. Wainwright, and John D. Lafferty, *High-dimensional Ising model selection using $\ell - 1$ -regularized logistic regression*, 2010.

- Guillem Rigai, Julien Chiquet, Martina Sundqvist, Valentin Dervieux, and Florent Bersani, *aricode*, <https://CRAN.R-project.org/package=aricode>
- Edmond Sanou, Christophe Ambroise and Geneviève Robin, *Inference of Multiscale Gaussian Graphical Models*, CompuTo, French Statistical Society
- RGS Soares, PA Ferreira, and LE Lopes, *Can plant-pollinator network metrics indicate environmental quality?*, *Ecological Indicators*, volume 78, pages 361–370, Elsevier, 2017.
- M.A. Sustik and B. Calderhead, *GLASSOFAST: an efficient GLASSO implementation*, UTCS Technical Report TR-12-29, University of Texas at Austin, 2012.
- Kean Ming Tan, Palma London, Karthik Mohan, Su-In Lee, Maryam Fazel, and Daniela Witten, *Learning graphical models with hubs*, arXiv preprint arXiv:1402.7349, 2014.
- Kean Ming Tan, Daniela Witten, and Ali Shojaie, *The cluster Graphical-Lasso for improved estimation of Gaussian graphical models*, *Computational Statistics & Data Analysis*, volume 85, pages 23–36, Elsevier, 2015.
- Martin J. Wainwright and Michael I. Jordan, *Graphical models, exponential families, and variational inference*, *Foundations and Trends® in Machine Learning*, volume 1, number 1–2, pages 1–305, Now Publishers, Inc., 2008.
- Joe Whittaker, *Graphical models in applied multivariate statistics*, Wiley Publishing, 2009.
- Shiqing Yu, Mathias Drton, and Ali Shojaie, *Directed graphical models and causal discovery for zero-inflated data*, *Conference on Causal Learning and Reasoning*, PMLR, 2023, pages 27–67.
- G. Yu, C. Gao, *enrichplot: Visualization of Functional Enrichment Result*, <https://yulab-smu.top/biomedical-knowledge-mining-book/>.
- G. Yu, L. Wang, Y. Han Y and Q. He. *clusterProfiler: an R package for comparing biological themes among gene clusters.*, *OMICS: A Journal of Integrative Biology*, 16(5), 284-287. doi:10.1089/omi.2011.0118, 2012.
- Xiangtian Yu, Tao Zeng, Xiangdong Wang, Guojun Li, and Luonan Chen, *Unravelling personalized dysfunctional gene network of complex diseases based on differential network model*, *Journal of translational medicine*, volume 13, pages 1–13, 2015, Springer.
- M. Yuan and Y. Lin, *Model selection and estimation in the Gaussian graphical model*, *Biometrika*, 94(1), 19–35, 2007.